GENERAL ATOMIC
DIVISION OF GENERAL DYNAMICS

GA-6094

FALLOUT STUDIES
CLOUD CHEMISTRY

FINAL REPORT

Subtask 3111A
Contract OCD-PS-64-222
Office of Civil Defense
Office of the Secretary of the Army
Department of the Army

January 29, 1965

GENERAL ATOMIC
DIVISION OF
GENERAL DYNAMICS

JOHN JAY HOPKINS LABORATORY FOR PURE AND APPLIED SCIENCE

P.O. BOX 608, SAN DIEGO, CALIFORNIA 92112

GA-6094

FALLOUT STUDIES
CLOUD CHEMISTRY

FINAL REPORT

Subtask 3111A
Contract OCD-PS-64-222
Office of Civil Defense
Office of the Secretary of the Army
Department of the Army

Work done by:

J. H. Norman
P. Winchell
W. E. Bell
A. B. Riedinger
H. G. Staley
M. Kirkbride
M. Tagami
G. Graves

Report written by:

J. H. Norman
P. Winchell
W. E. Bell
A. B. Riedinger

January 29, 1965

ABSTRACT

The measured absorptions per atmosphere between 1260° and 1400°C of Cs, Ru, Sb, Te, and Mo in $CaO-Al_2O_3-SiO_2$ samples with varying SiO_2 content are, respectively, 10^3 to 10^5, 10, 10^4, 10^0, and 10^5 to 10^4 times the ideal values as calculated by Miller. These measurements were made by equilibrating fission-product-containing oxygen with the various silicates at the experimental temperature. When cesium was used in this type of experiment, some anomalous behavior was noted. Attention is called to the effect of gaseous ions on chemistry occurring during fallout formation.

Diffusivities of Cs, Sb, Te, and Mo are reported as determined in diffusion-limited evaporation studies and plane-source-technique studies. Values of measured diffusivities are such as to suggest that condensed-state diffusion of the moderately volatile fission products should be important in fallout formation. Variation of diffusivity of Sb with silicate composition was studied.

Mass-spectrometric studies of the thermodynamics of vaporization of the alkaline earth oxides are reported. Gaseous species whose thermodynamic properties are reported here were found to include M, MO, M_2O, and M_2O_2 species.

Microprobe studies of fallout particles revealed concentration gradients for many elements in fallout particles. These studies clearly portrayed accretion events occurring in the first few seconds after a nuclear event.

A discussion is presented of the importance of thermodynamic properties of fission products and silicates and the kinetics associated with the fission-product absorption process, with particular emphasis on condensed-state diffusion and particle accretion events.

CONTENTS

I. INTRODUCTION

The program carried out at General Atomic for the elucidation of chemical phenomena associated with the formation of fallout particles has generally followed five lines of endeavor:

1. A study of high-temperature silicate absorption of fission products under equilibrium conditions has been performed.

2. Evaluation of diffusion coefficients for important fission products in molten silicates by both ordinary and novel techniques has been accomplished.

3. Mass spectrometric investigations of gaseous species and associated thermodynamics for fission-product oxides and major soil constituents have been performed.

4. A study, using electron microprobe apparatus, of how various elements are distributed in actual fallout particles has been initiated.

5. Consideration has been given to how the phenomena observed might fit into the process of fallout formation.

It is believed that information derived from this work has led to an improved understanding of how fallout particles form following a nuclear detonation and how fission-product elements are distributed in the fallout particles. This report includes a description of these studies and ideas and also includes our interpretation of areas where further studies would enhance the knowledge available for the development of a complete model for fallout formation.

II. EQUILIBRATION STUDIES

GENERAL TECHNIQUES

In the last formal report[1] by this group, a description of an equilibration system to measure absorption of fission products in silicates was presented. Since that presentation, the system has been used to measure the absorption of Te, Sb, Mo, and Cs in silicates (a similar technique has been used to measure Ru absorption). The apparatus, shown in Fig. 1, consists of two fairly close-fitting, counter-current-flow platinum tubes. The outside tube is closed at the bottom and the inside tube has a capillary tube as its base. The region between the capillary and the bottom of the outside tube is held at a known temperature. Silicate samples are placed in this region, where they absorb a radioisotopically labeled element from the gas phase. This element is added to the gas flowing in this region as a result of the presence of a silicate melt containing the element. This source melt is about 1000 times as massive as the silicate samples. The system is operated at elevated temperatures until the samples are equilibrated with the flowing ambient gas phase. Then the amount of element in the flowing gas phase is measured by trapping and measuring the amount of radioisotope per unit volume of gas passing through the capillary. This affords a partial-pressure measurement, as the carrier gas is passed at a known flow rate through the system at one atmosphere. The system is quenched as rapidly as feasible ($\sim 30^{\circ}$/sec). The system is then disassembled and the amount of radioisotope in the silicate samples determined. The element pressure and absorption data as a function of temperature and silicate and gas phase composition then can be used in describing the thermodynamics of the absorption process. Data are reported in terms of grams of element per gram of silicate per atmosphere pressure of the element in the gas phase.

Silicate samples used in the study have been prepared at General Atomic by melting the ingredients together, grinding, sieving (200 mesh), and remelting the glasses formed from CaO, SiO_2, and Al_2O_3. One of these glasses is of eutectic CaO-Al_2O_3-SiO_2 composition; the others are of this composition with more or less SiO_2. The five sample glasses have a 3 CaO/Al_2O_3 mole ratio of 0.98 ±0.05 and equivalent mole ratios for $SiO_2/(CaO + 1/3\ Al_2O_3 + SiO_2)$ of 0.3430, 0.4484, 0.5483, 0.6334, and 0.7630. The compositions of these samples are demonstrated in the partial CaO-SiO_2-Al_2O_3 liquidus surface diagram shown in Fig. 2.

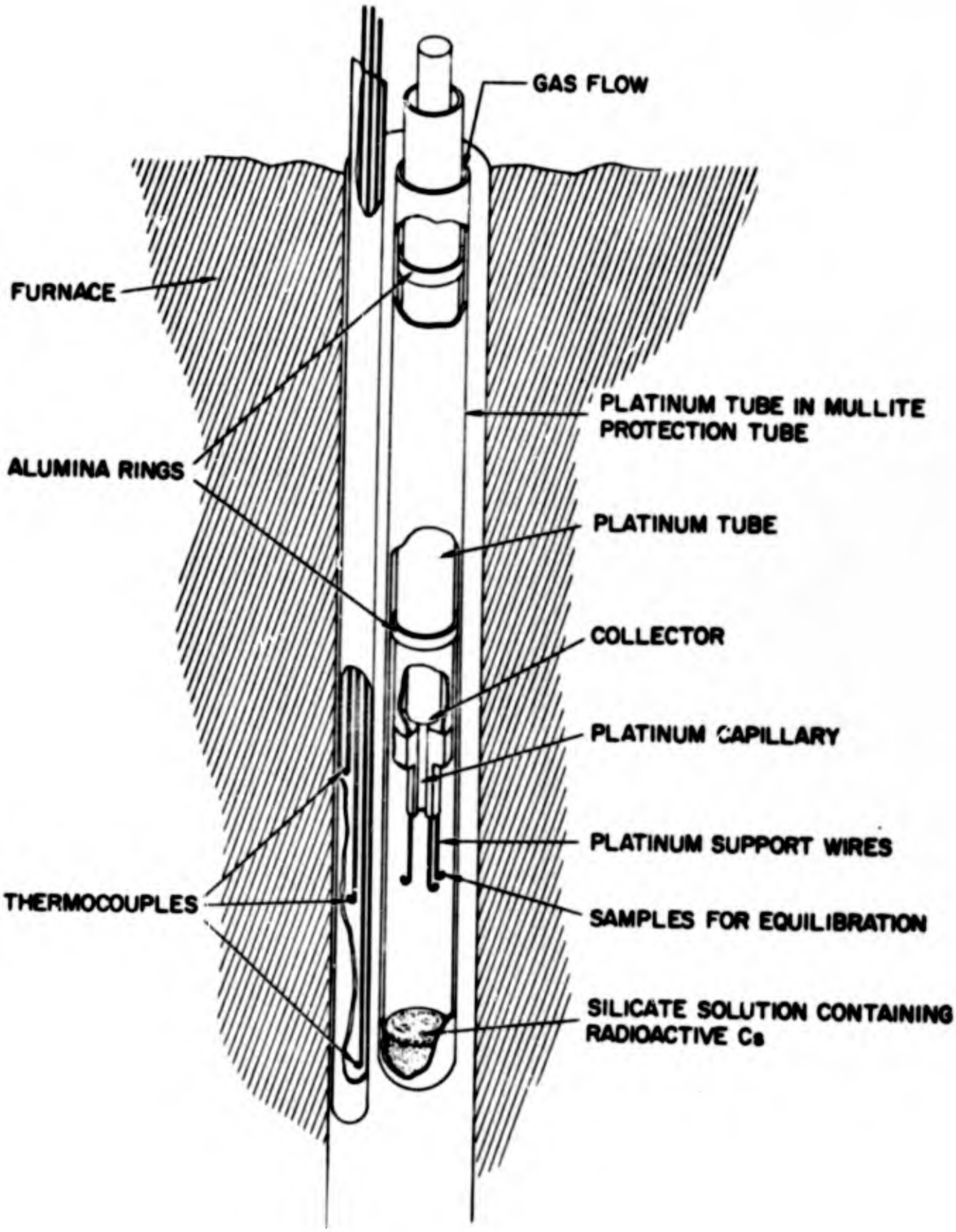

Fig. 1--Equilibration apparatus

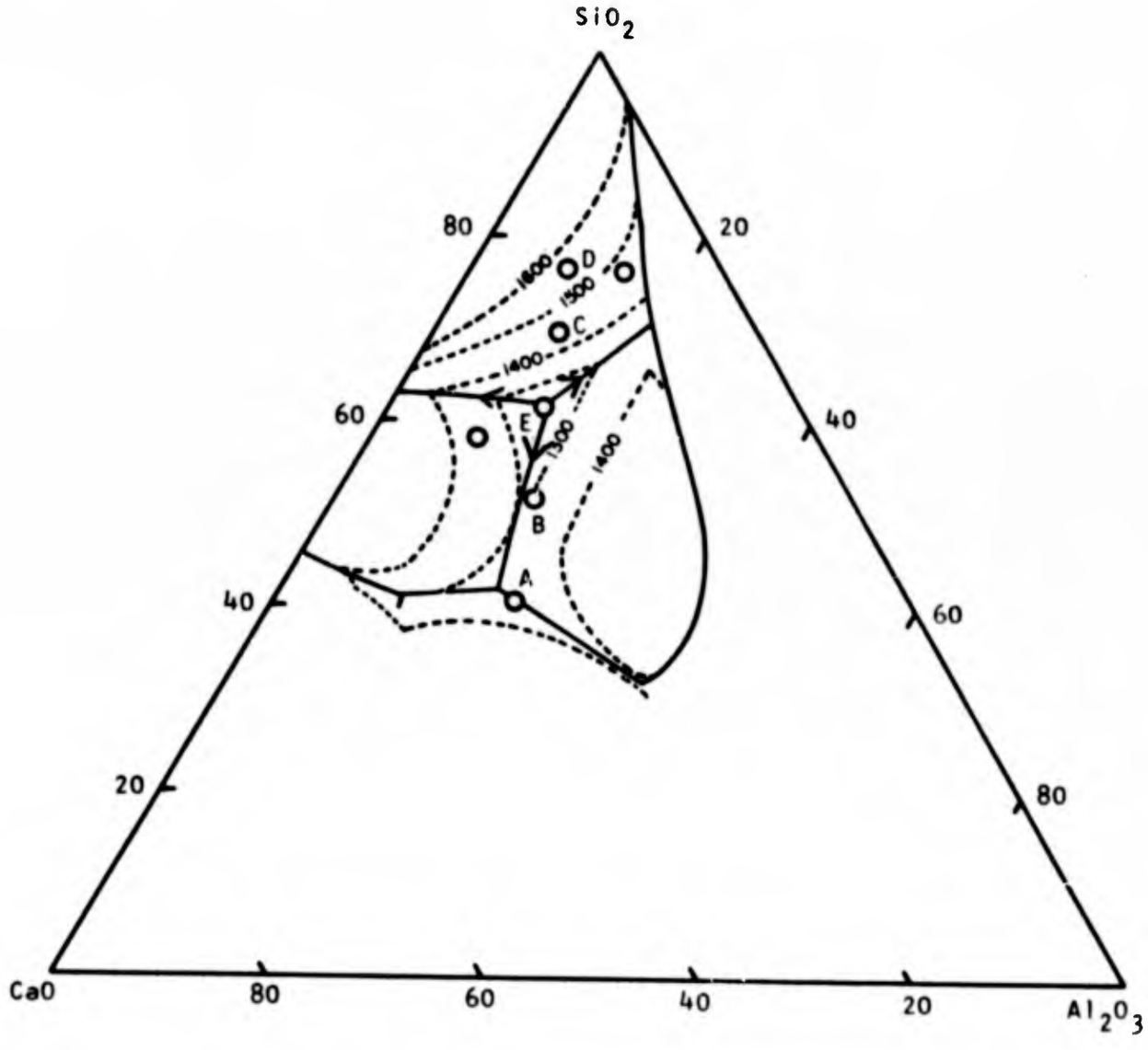

Fig. 2--Liquidus surface diagram of $CaO-Al_2O_3-SiO_2$ (temperature in ^oC)

The experimental systems will now be considered individually.

Molybdenum-Oxygen System

For use in studies of molybdenum absorption in silicates from an oxygen atmosphere, 10 millicuries of 66-hr Mo^{99} in ammoniacal ammonium molybdate containing 6.52 mg Mo was purchased from Oak Ridge National Laboratory. The solution as-received was mixed with a blended powder consisting of CaO, Al_2O_3, SiO_2, and a small amount of eutectic glass such that the powder was of $CaO-Al_2O_3-SiO_2$ eutectic composition. The moisture was evaporated slowly from the mixture to avoid mechanical or evaporation loss of molybdenum. The resulting mass was transferred to a platinum tube and rapidly heated to a melting temperature. (The CaO suppressed MoO_3 evaporation by forming $CaMoO_4$.) This melt then was used as a source melt for molybdenum oxide vapor.

In preliminary experiments it was found that a quartz condensing tube was satisfactory for catching the molybdenum vapors in the cooler furnace regions (the daughter Tc^{99} vapors, however, are not so successfully contained). In these experiments a close-fitting quartz tube was inserted into the inner platinum tube, where it served as the gas-flow tube as well as the condensing tube. This tube could be changed without cooling the system appreciably. Following removal of a tube it was sectioned and counted at 0.64 Mev to 0.84 Mev for the Mo 0.74 Mev γ. The silicate samples were also counted in this energy band. Absorptions obtained in these studies ranged from 0.7 to 0.04 wt-% Mo. The absorption per atmosphere data from these experiments are presented in Fig. 3 as a function of temperature.

Although no major chemical or physical problems were noted during the experiment, the system is certainly not conducive to leisurely study. The short molybdenum half-life requires that data from one source be acquired in a few weeks.

Calculations on available dimerization and trimerization thermodynamics for MoO_3[2] in the observed pressure ranges for Mo indicate that MoO_3 is the only gas species that need be considered. From Miller's tables[3] MoO_3 (g) is represented as having a heat of vaporization from liquid MoO_3 of 81.5 kcal/mole. The heat of absorption from this study is -67.5 kcal/mole. For ideal behavior of this system, these two numbers should be equal in magnitude and opposite in sign. The -67.5 value would then indicate a lowering of the heat of vaporization for MoO_3 (ℓ) dissolved in the silicate. However, according to the MoO_3 (ℓ) vaporization thermodynamics given in Miller's tables, the activity coefficient of MoO_3 (ℓ) appears to have been also lowered by solution in silicate. These data are not contradictory, but

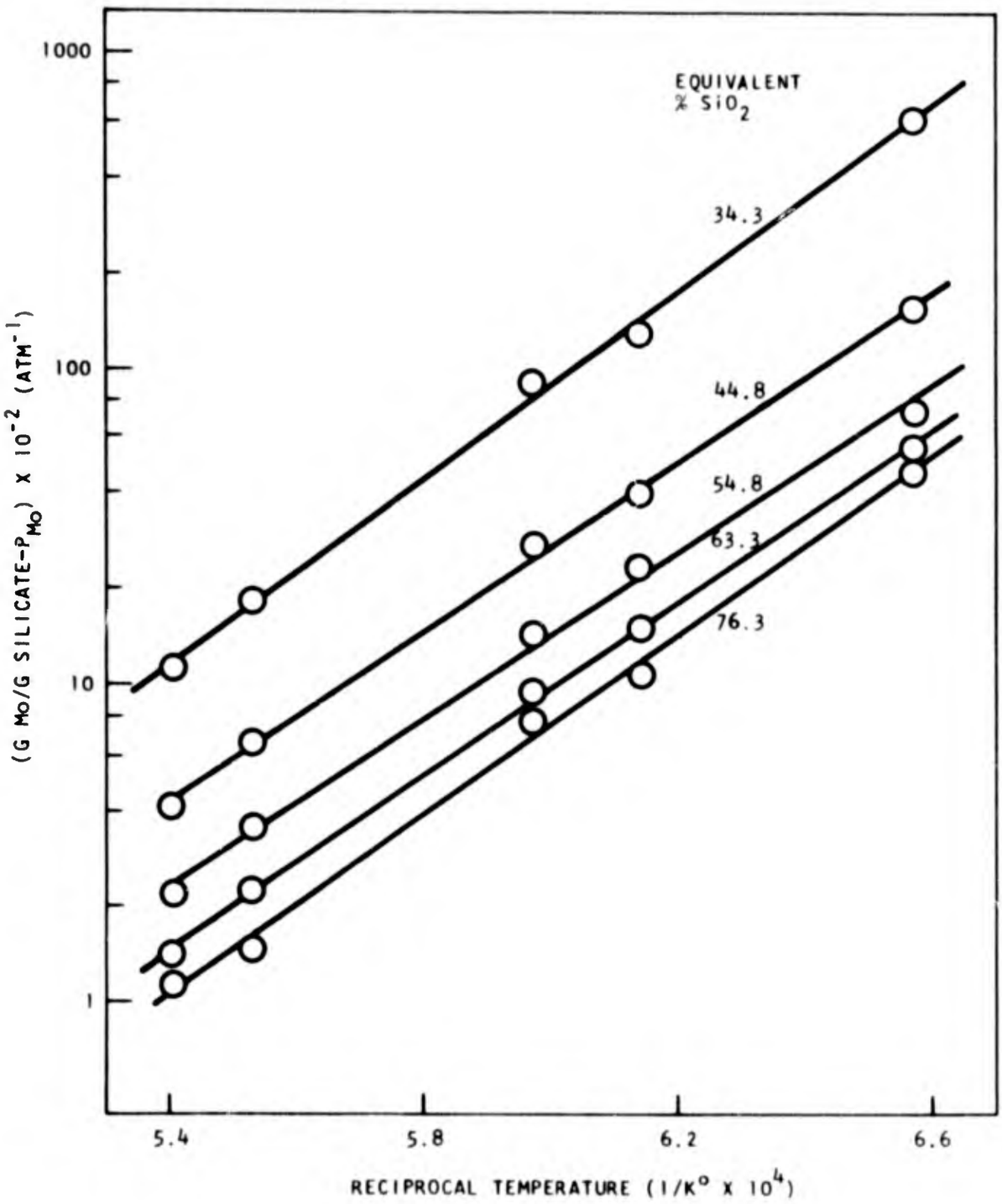

Fig. 3--Experimental molybdenum absorption on various silicates as a function of temperature

it is unusual for the activity coefficient to decrease appreciably when the heat of vaporization decreases appreciably. This subject will be considered later.

Tellurium-Oxygen System

The experimental procedure used in this study closely paralleled that of the molybdenum study. The source melt was composed of 5.23 g of near-eutectic $CaO-Al_2O_3-SiO_2$ (61.6% SiO_2 instead of 62.0%) from the metal oxides and 16.3 mg of TeO_2 containing 104-day Te^{123} obtained from Oak Ridge. This study has been only partially successful. In this case absorption of tellurium was too low to be properly measured. Absorptions were around 2 to 4 counts per minute per milligram of silicate, so that even with nearly 10 mg of silicate sample the counting rates were quite low. The tellurium absorption results obtained in this cursory study are presented in Fig. 4 together with a comparison of molybdenum and other data. No satisfactory temperature variation data were obtained. In future studies, tellurium absorption might better be studied at lower temperatures with low melting silicates and a more prolific source.

Antimony-Oxygen System

This system was essentially that used for molybdenum. The source sample was prepared in essentially the same way as the molybdenum source. The 2.7-year Sb^{125} (obtained from Oak Ridge) was diluted with 12.1 mg of Sb_2O_3 which was then put into 4.38 g of $CaO-Al_2O_3-SiO_2$ eutectic. The study, however, was quite superficial, since it was quickly discovered that even in the oxygen atmosphere antimony was absorbed to a large extent in platinum. The vapor pressures of the antimony measured by passing the transpiration gases through the platinum capillary may not be applicable to the gases in the equilibration region because of the Sb-Pt interaction. Also, the platinum sample holders absorbed one-tenth the antimony absorbed by the silicate. Both of these effects, with particular emphasis on the former, lead one to attach a moderate degree of uncertainty to the antimony data. The data, with the stated reservations, are summarized by the antimony curve presented in Fig. 4. No heat of absorption was obtained from this study.

Ruthenium-Oxygen System

The absorption of ruthenium oxide vapor by silicate samples has been measured, using mullite equilibration apparatus. Like antimony and tellurium, absorption, the results given in Fig. 4 show that variation in silicate composition has relatively little effect on the degree of ruthenium absorption.

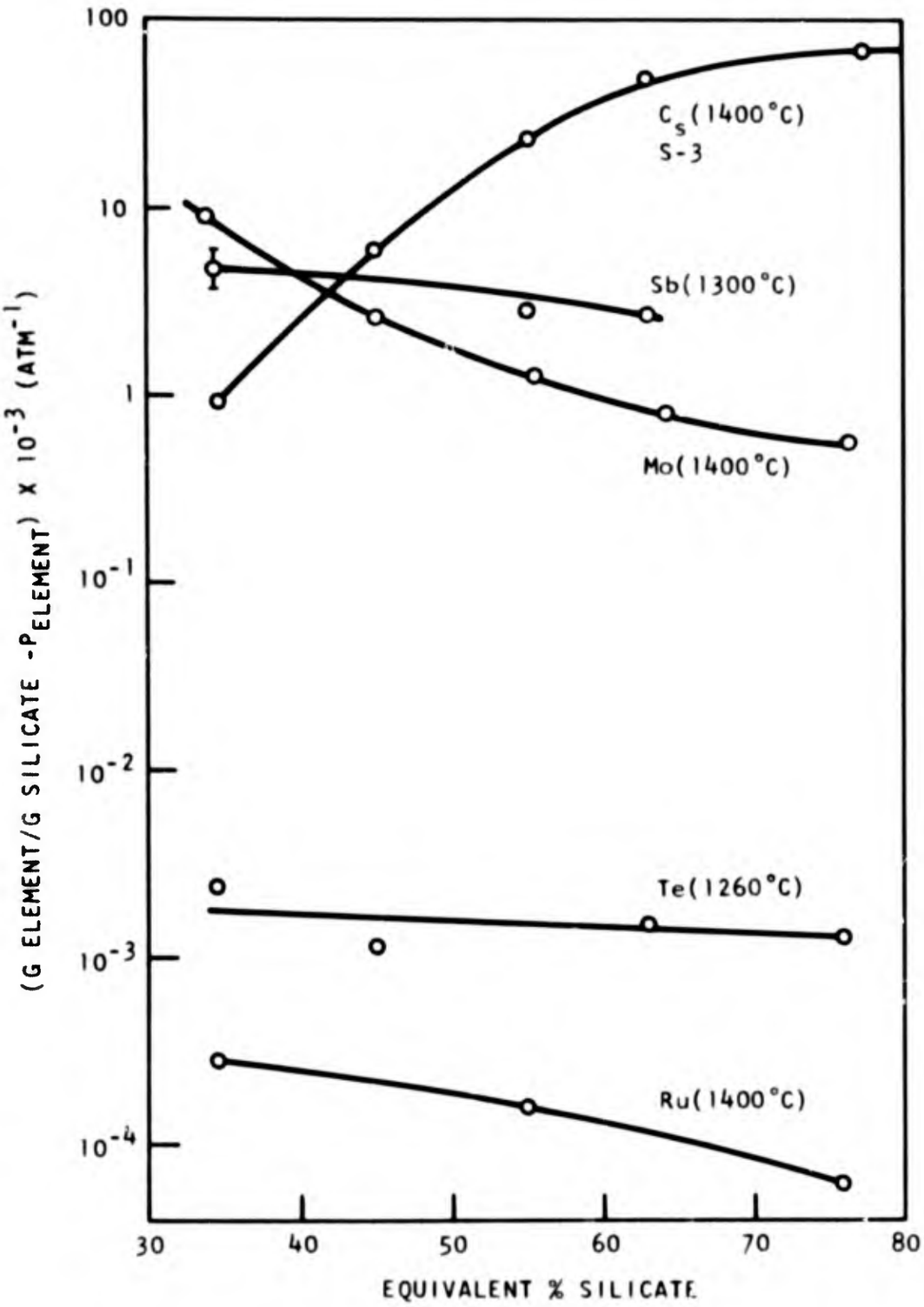

Fig. 4--"Henry's law constants" for Cs, Pb, Mo, Te, and Ru

Mullite apparatus similar to that employed by Bell and Tagami [4] was used in this work because it was known from previous experience that this material would not absorb ruthenium to an appreciable extent at temperatures up to 1500°C.

In this work, carrier-free 1-year Ru^{106} (5 mc) in the form of an aqueous chloride solution (obtained from ORNL) was added to an aqueous chloride solution containing about 90 mg of carrier ruthenium. The resulting solution was evaporated to dryness in a small mullite boat with a heat lamp. The dried chloride was reduced to metal with hydrogen at 600°C. Silicate samples (~0.5 mg) were fused onto a small piece of platinum foil. It was realized that the platinum would absorb ruthenium to a relatively high degree, but such a material was necessary to avoid interaction with the silicate samples.

The platinum foil holding the silicate samples and the mullite boat, which contains the radioactive ruthenium metal, were placed about 1 in. apart in a mullite protection tube of about 0.8 cm ID. The source sample region and the tube were placed in an isothermal region of a high-temperature furnace. Mullite diffusion barriers were used both upstream and downstream. Oxygen at 1 atm pressure was slowly passed through the protection tube, and the silicate samples were allowed to equilibrate with the ruthenium oxide (RuO_3 and RuO_4) vapor. The silicate samples were withdrawn (quenched) from the system periodically and counted to follow the approach to equilibrium. It was, of course, necessary to remove the silicate samples from the platinum foil when the counting was done, since the platinum absorbed more ruthenium than did the samples. It was believed that because of the approach to apparent equilibrium conditions the presence of the platinum did not greatly affect the ruthenium partial pressures. "Henry's law constants" were calculated utilizing the absorption data and ruthenium oxide vapor-pressure data. The latter were derived from the previous work of Bell and Tagami[4]

Cesium-Oxygen System

Most of the work on equilibration of fission products with silicates has been concerned with cesium studies. In our previous report,[1] we stated that slow diffusion of cesium might well be the cause of the failure of transpiration studies to produce consistent results. We cited behavior of the system toward varying flow rates, some measured inhomogeneities in source melts, and the lack of sensitivity to changes in carrier gas as possibly being explainable on the basis of lack of attainment of equilibrium. We explained these effects on the basis of slow diffusion of cesium in the molten glass source. We have since measured the diffusion coefficient of cesium in this glass, however, and calculations on the basis of our measured diffusion coefficients of 10^{-7} cm^2/sec at 1400°C, the source

thickness, and measured rates of evaporation of cesium from this source do not support this hypothesis. The rate of evaporation from the source would appear to be a couple of orders of magnitude too low for diffusion-controlled evaporation. It would appear, therefore, that slow condensed-phase diffusion would not explain inconsistent results obtained in transpiration studies.

In the last report, the equilibration apparatus and counting methods were described as they apply to cesium studies. The apparatus differs from that used in the molybdenum experiments only in that cesium is caught on a hot mullite rod instead of in a quartz tube.

One of the first problems encountered in the cesium studies was that of inhomogeneity of silicate samples on the milligram or less scale. This problem was solved by using powdered ingredients, melted, powdered, and remelted as described. Cesium absorption on samples of these remelted silicates varies by about ±20%, with some of the uncertainty being in the weights of the samples. Using these samples, we have studied absorption of cesium tagged with Cs^{134}, both prepared at General Atomic and obtained from Oak Ridge, from three different source melts. The source melts of two of these (S-2 and S-3) were initially 5.20% Cs, while the third (S-1) was 0.115% Cs. However, Cs^{134} content in S-1 was somewhat higher than that in the other two samples. For the low-cesium-content source and one of the other sources (S-2), eutectic $CaO-Al_2O_3-SiO_2$ was used as a solvent. The remaining source (S-3) melt had a significantly higher $(CaO + 1/3\ Al_2O_3)/SiO_2$ ratio and exhibited the highest cesium partial pressures.

The results of cesium equilibration at 1400°C with the various sources are shown in Fig. 5. The three absorption curves shown in this figure do not appear to be the same according to statistical treatments of the data, although the difference between curves is not great; that is, the curves are quite similar and the magnitudes at a given equivalent % SiO_2 vary only within a factor of ten. The results are believed to apply well to the silicates as used--that is, matrix redistribution in the system was negligible--since the absorptions were not time dependent as would be expected for a redistributing system. This data, then, might, on its face, be taken as an indication of lack of agreement with Henry's law. However, since the data is not monotonic with cesium pressure (cesium pressures range from 2×10^{-6} atm for S-3 to 1×10^{-7} atm for S-1) this conclusion should not be drawn. We have no satisfactory explanation of why this data varies as it does.

The temperature coefficients of the absorptions per atmosphere (using the data from the high-specific-activity cesium silicate source) are plotted against reciprocal temperature in Fig. 6. It has been our opinion that the thermodynamics of vaporization of cesium from the silicate

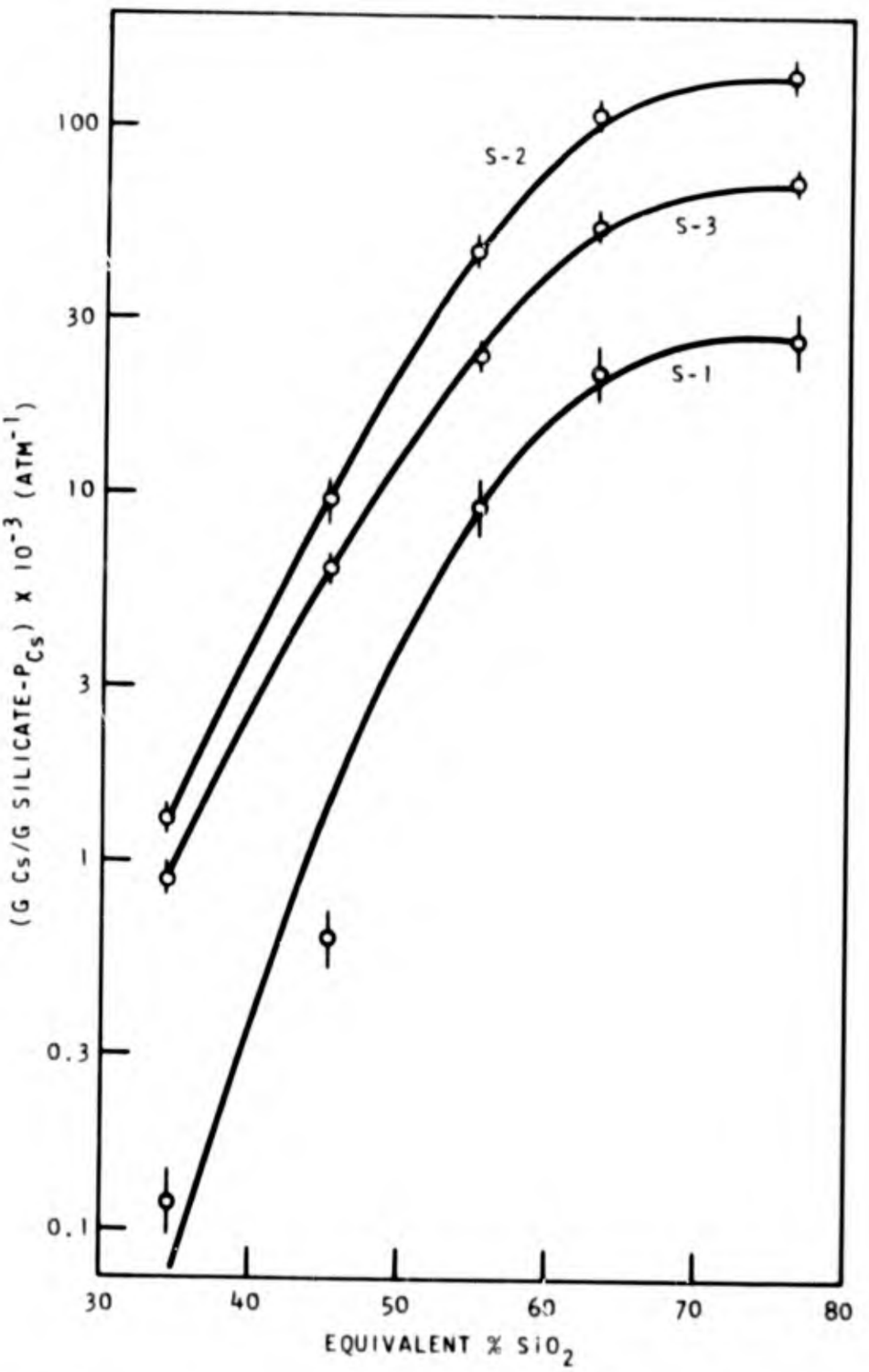

Fig. 5--Calculated "Henry's law constant" for cesium ($1400^{\circ}C$; 1 atm O_2)

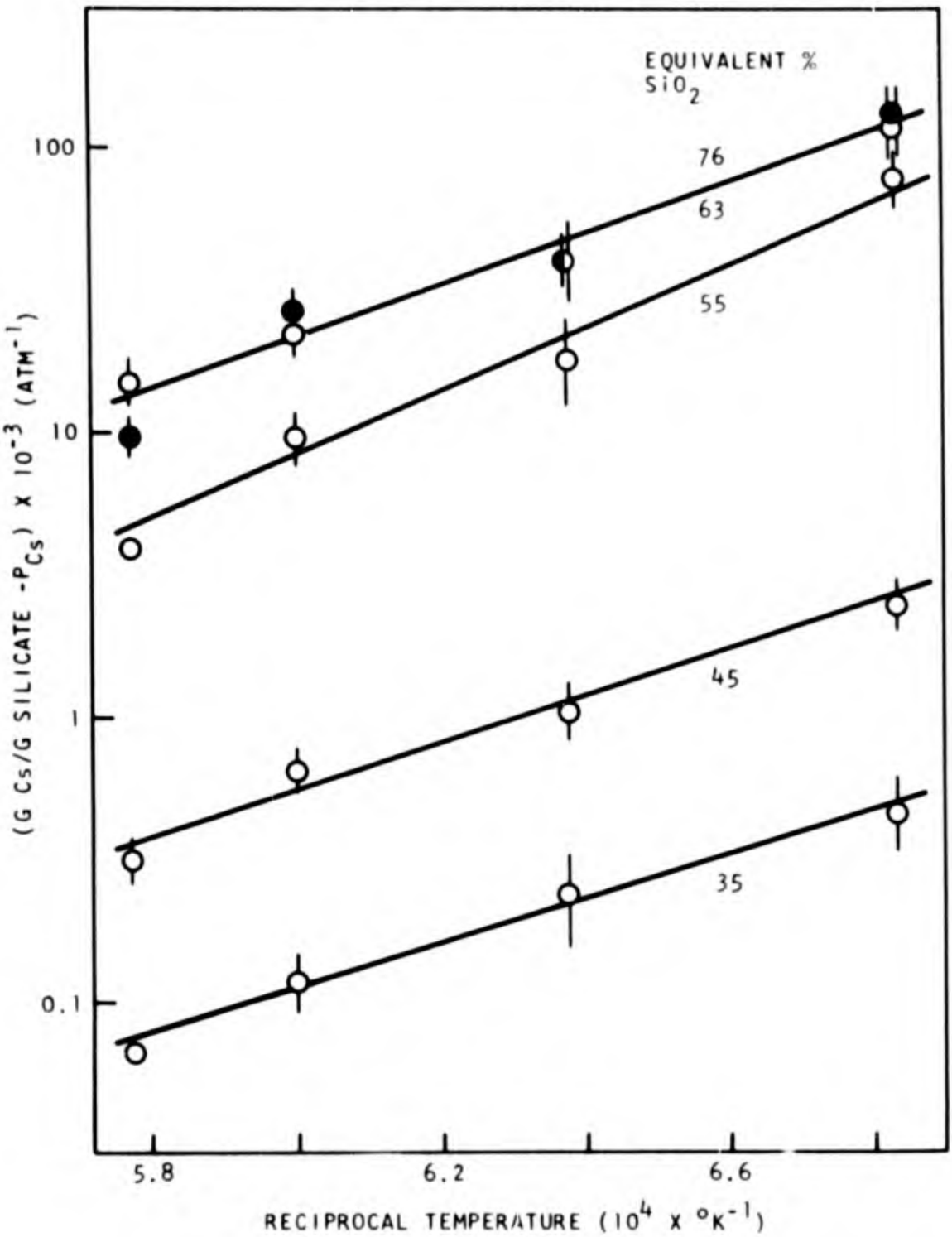

Fig. 6--Temperature dependence of "Henry's law constant" for cesium

could be interpreted in terms of a two-step process: (1) the condensation of gaseous cesium to liquid cesium oxide and (2) the dissolution of liquid cesium oxide in the silicate. From Coughlin,[5] the heat of condensation of cesium gas to liquid cesium oxide in an oxygen atmosphere is estimated as -56 kcal/mole. One would at first anticipate that liquid cesium oxide would dissolve exothermically in the silicate. This means that the heat of the "Henry's law constant," the temperature coefficient of the absorption per atmosphere calculated from Fig. 6, would be expected to be less than -56 kcal/mole Cs. The temperature coefficient for all five silicates grouped is -41 ±5 kcal/mole, or somewhat more than the -56 kcal/mole for condensation to liquid cesium oxide. It would appear, then, that these results cannot be interpreted on a sound thermodynamic basis. This is not unexpected. If the "Henry's law constant" is not constant with varying conditions, as indicated in Fig. 5, it is not surprising that its measured temperature coefficient is not interpretable in terms of simple thermodynamic quantities corresponding to the expected reaction.

The question of what might be causing trouble in the equilibration method leads back to the fact that a reaction quenching method is being used in the analysis. Inadequate quenching, at least, can be called upon to explain why the temperature coefficient of the "Henry's law constant" for cesium (and other systems) might be low. Data from high-temperature experiments might be expected to pertain to a lower temperature if a quench were inadequate. However, the lower the study temperature the less would be the quenching error, since diffusivities decrease rapidly with decreasing temperature. With this in mind, experiments were designed to obtain absorption data without quenching.

DYNAMIC EQUILIBRATION STUDIES

An apparatus was set up to measure "Henry's law constant," at high temperature for cesium in silicates, using a transpiration-type technique. The apparatus was arranged such that equilibrium could be approached both by absorption and desorption, the concentration of cesium being determined in situ. By this approach, it was hoped that difficulties such as diffusion or evaporation limiting conditions and possible errors due to quenching of the sample would be avoided.

The apparatus for this study is shown schematically in Fig. 7. An 0.078-g sample of CaO-Al_2O_3-SiO_2 glass of eutectic composition was placed in a 2.8 mm by 10.6 mm platinum boat. The boat was placed inside a 7-mm platinum tube that had been welded to a gold tube. Cesium nitrate, tagged with Cs^{137}, was placed in a gold boat in the gold tube. This assembly was placed in a compound furnace so that the temperature of the cesium nitrate source and the silicate specimen could be controlled

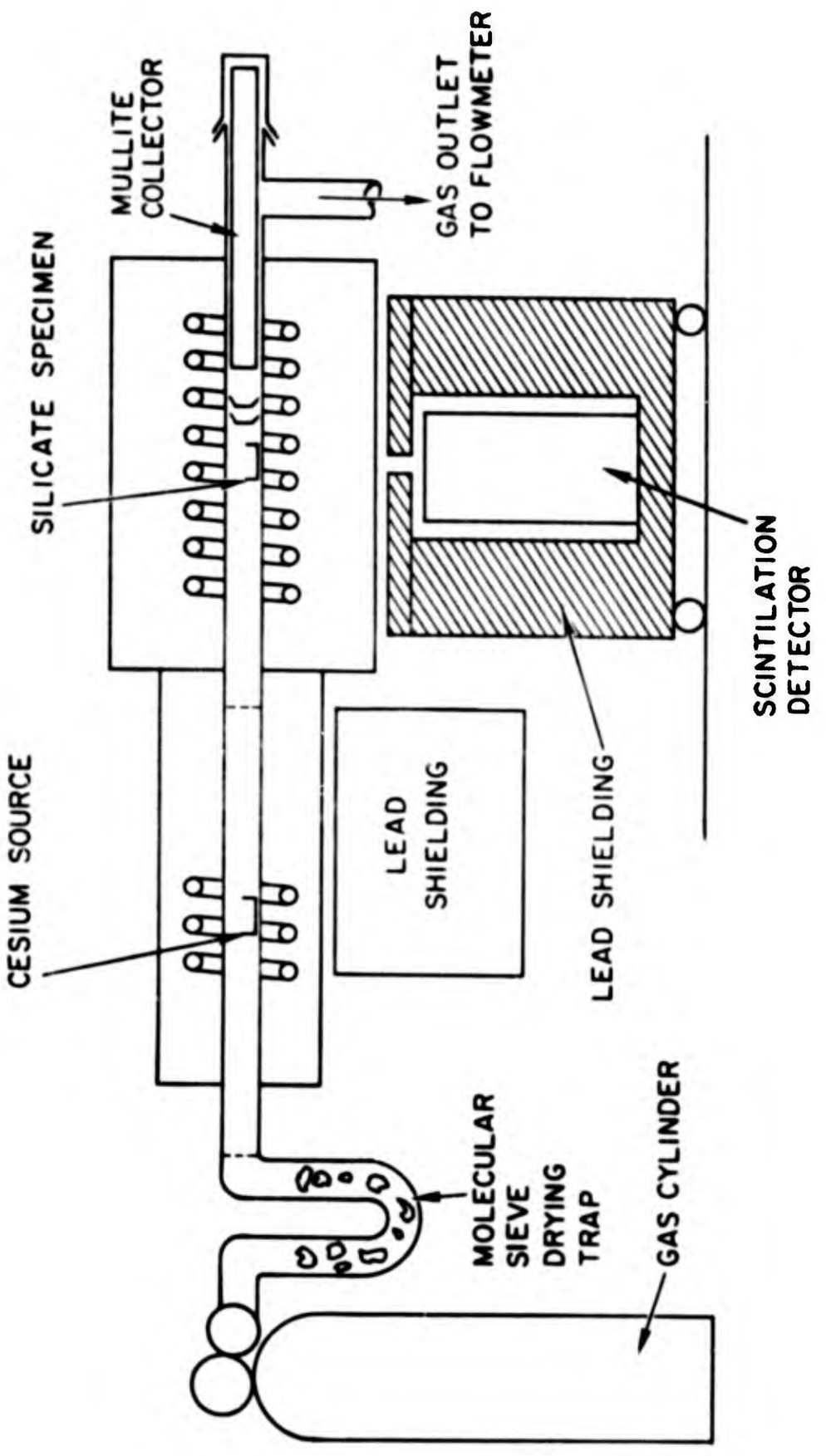

Fig. 7--Dynamic equilibration apparatus

independently. Oxygen, or argon, which had been passed through a molecular sieve drying trap was allowed to flow through the tube. A removable mullite tube was inserted in the platinum tube downstream of the silicate to collect cesium vapor. The cesium nitrate was decomposed to an oxide by heating and then was used as a source to produce a cesium pressure in the gas stream. A collimated gamma-ray scintillation detector mounted under the silicate sample was used to determine the quantity of cesium absorbed by the silicate sample. This detector could be moved to scan the tube, both to locate the specimen and to determine the background. Periodically, a mullite collector was withdrawn (and replaced with a new one) and counted in a well-type gamma-ray scintillation detector. The vapor pressure was calculated from the amount of cesium collected on the mullite and the gas-flow volume.

Absorptions per atmosphere cesium pressure obtained in the $CaO-Al_2O_3-SiO_2$ melt of eutectic composition in an oxygen atmosphere over the temperature range of 1300° to 1430°C are shown in Fig. 8. The heat was found to be -78 ±5 kcal/mole--a number quite acceptable theoretically. The solid circles designate points obtained from desorbing cesium and the open circles designate points obtained from absorbing cesium. The cesium concentration for these points was 1.4% to 4.5%. Apparent equilibrium points, using argon as a sweep gas instead of oxygen, gave higher absorptions per atmosphere--as shown by the open squares on Fig. 8. The reason for the increase rather than the expected decrease in absorption per atmosphere cesium pressure in argon is not known, but the same unexplained effect has been noted in some of our other studies.

Measurements by the same technique are progressing, using the $CaO-Al_2O_3-SiO_2$ melt of composition 34.3 equiv.-% SiO_2. An absorption per atmosphere has been found at 1340°C, which is approximately a factor of 100 less than for the eutectic. This is in agreement with the results obtained with the quenched microsamples. Additional studies are aimed at obtaining a heat of absorption and more information on the dependence on absorption in other gases.

Although the advantage of determining absorption in situ seems great, studies of this type are very time consuming; one must wait for the large sample employed to come to equilibrium, and data for only one silicate can be obtained in an experimental setup at one time. For reasons of time economy, this method cannot easily be considered a universal study method for obtaining thermodynamics for fallout systems.

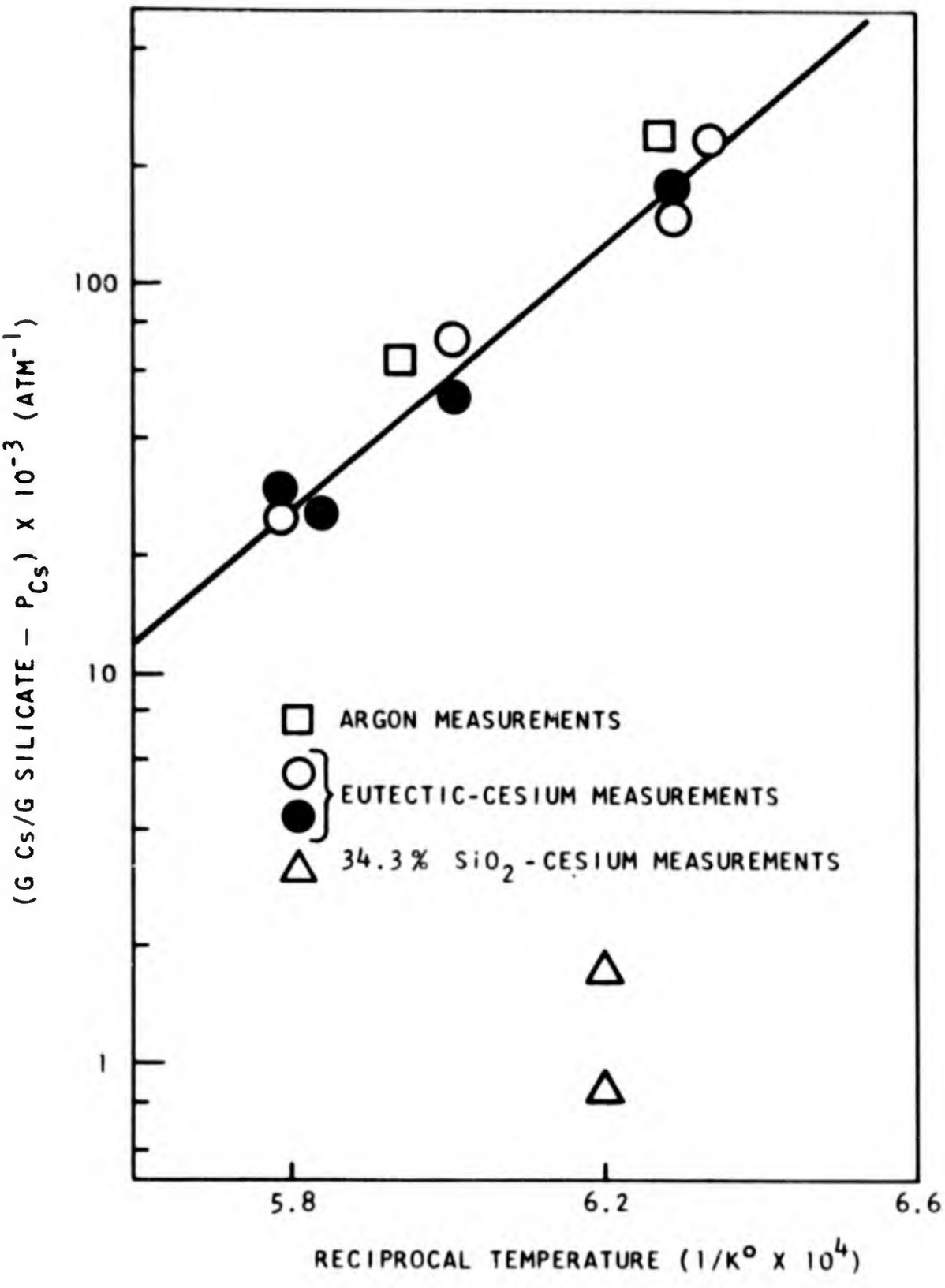

Fig. 8--Dynamic equilibration absorption per atmosphere cesium under various conditions

CESIUM-ARGON SYSTEM

Using the quenching equilibration system, the results with argon as the carrier gas are not experimentally different from those with oxygen as a carrier. As reported previously, the argon results in the dynamic system differ only slightly. The transpiration results reported previously[1] also indicate no argon sensitivity. In all cases, efforts have been made to ensure very low water content in the systems. We have considered that the absorption of cesium could be described by the following reaction:

$$Cs(g) + 1/4\ O_2 + 1/2\ SiO_2(sol.) \rightleftarrows Cs^+(sol.) + 1/2\ SiO_3^=(sol.)\ .$$

On the basis of this reaction the degree of cesium absorption should decrease on changing from oxygen to argon. This reaction, however, seems to be questionable on the basis of experimental results. The results are in line with Cs_2O as the evaporating species, not $Cs + 1/4\ O_2$. We have observed Cs(g) evaporating from glasses mass spectrometrically--we have never observed $Cs_2O(g)$. It seems questionable that $Cs_2O(g)$ will be found.[6] The lack of effect of argon is unexplained at this time even though it is well established. Further studies will be directed toward solving this problem.

CESIUM-DATA EVALUATION

The results of all the cesium studies performed--quenching equilibration studies, dynamic equilibration studies, and transpiration studies at low flow rates--give absorptions per atmosphere for cesium of about the same magnitude, 10^4 grams of cesium per gram of eutectic silicate per atmosphere at 1400°C. There seems little doubt that this is a good experimental value. Also, the quenching and dynamic equilibration apparatus give the same numbers for the 34 equivalent percent SiO_2 silicate sample. The major questions then are, what is the proper temperature coefficeint of this property and what is the precise chemical reaction to which this value pertains. A continued effort to unravel these problems is anticipated.

One procedure that has worked quite well in two tests is that of using the equivalent percent SiO_2 to represent the composition of a sample. Two samples were prepared with 3 CaO/Al_2O_3 ratios of 1.94 and 0.385 instead of the normal 0.98 ±0.05. Measured cesium absorptions were in line with the cesium absorption of the other samples of the same equivalent % SiO_2. That is, to a first approximation the CaO/Al_2O_3 ratio of the solvent can be ignored.

SOME CONSIDERATIONS OF THE ROLE OF IONS IN FALLOUT FORMATION

The existence of gaseous ions, independent of their own chemical properties, affects the partial pressures previously assigned to neutral gas phase components in our studies. For instance, let us consider the case of the reported cesium absorption studies. In these studies, the only cesium species in the gas phase was taken to be monatomic cesium. It is apparent, however, that cesium ions should be considered. The behavior of the gaseous system $Cs\text{-}Cs^{+}\text{-}e^{-}$-air may be described as follows.

The cesium ion partial pressure decreases with the square root of the cesium atom partial pressure until the cesium ion partial pressure becomes somewhat smaller than the ambient electron partial pressure. From this point on, a more or less steady cesium-ion/cesium-atom ratio will be established. More quantitatively, this behavior is described by the Saha equation[21] and a condition of electrical neutrality applied to the gas phase components. The value for the equilibrium constant as obtained at 1600°C by applying the Saha equation to the following reaction,

$$Cs(g) \rightleftarrows Cs^{+}(g) + e^{-}(g) \quad ,$$

is $10^{-10.78}$. If no other ions are considered and the cesium atom partial pressure is $10^{-10.78}$ atm at 1600°K, the cesium ion and electron partial pressures are also $10^{-10.78}$ atm. These numbers might suggest that ions may not be particularly important in our experiments or for that matter in fallout formation. However, there are two phenomena that may greatly increase the importance of positive ions. These are (1) electron attachment reactions, which may considerably lower the electron partial pressures and, in accordance with the Saha equation, increase the cesium ion pressures, and (2) the presence of ionizing radiation from our tracers or from fission products during fallout formation, which may greatly increase the steady-state positive-ion partial pressures. Attachment reactions depend greatly on gas phase composition and are certainly important, but the ionizing radiation effect looks more important, at least in fallout formation. Estimated ion recombination rates are slow enough (~1 sec ion half life) and ionization rates are high enough (several per second per fission product atom) that an increase by several orders of magnitude in, for example, cesium-ion partial pressure over that given by the Saha expression might be expected for steady state during fallout formation. Even in our measuring systems using radioactive cesium, the gas phase ionization rate may be such as to appreciably alter the cesium-ion pressures. Therefore, we believe that whether or not gaseous ionization by nuclear radiation is important in fallout formation, it should certainly be considered. Possibly a

representation of steady-state electron temperatures might be attempted to help answer this question.

EVALUATION OF EQUILIBRATION DATA

The value of the data to the fallout model should be considered from two different points of view: (1) how does this data quantitatively affect the present fallout model calculations and (2) how accurately does this data describe the thermodynamics of the condensation and dissolution processes suggested in this report?

The answer to the first question can be made quite satisfactorily. Certainly these studies have pointed out that the composition of the solvents must be considered in describing the absorption of certain fission products. For example, cesium dissolution in the limited range of solvents employed in this study exhibited a hundredfold variation in absorption per atmosphere. Another factor is the variation of these data from the ideal solution behavior represented by Raoult's law constants at the same temperature suggested by Miller.[3] This information is presented for 1400°C in Table 1. These numbers are directly comparable and describe the difference between ideal and real dissolution data. Certainly in the cases of cesium, antimony, and molybdenum a large enough difference exists between real and ideal information to greatly alter the behavior of these elements in fallout calculations. In these cases, the data of this report are to be preferred over an assumed ideal behavior.

Table 1

A COMPARISON OF REAL AND THEORETICAL PRESSURES AT 1400°C

Element	Raoult's Law Constants According to Miller (atm)	Reciprocal "Henry's Law Constants" According to Fig. 4 (atm)
Cs	1.88	10^{-3} to 10^{-5}
Ru	1.14	3 to 10
Sb	1.84	4×10^{-4}
Te	4.94	0.6 to 1
Mo	13.32	10^{-3} to 10^{-4}

In contrast, since the data of this report are generally based on a quenching method, since temperature coefficient data are not well understood, and since behavior with different atmospheres and different concentrations also is not well understood, the data presented here must be considered only partially complete in a chemical thermodynamic sense. Certainly the goal of these studies is to obtain data that are complete and consistent thermodynamically.

III. DIFFUSION OF RADIONUCLIDES IN MOLTEN SILICATES

INTRODUCTION

In the course of this project, the importance of diffusion limitation in any realistic fallout model has been emphasized. Any model should include both kinetic (diffusion, condensation coefficient) effects and equilibrium (Henry's law) effects. An example of diffusion-controlled transport in a real case can be demonstrated. A fallout particle was sectioned and studied, using an electron microprobe. A concentration gradient of lead was observed in the specimen; the profile is shown in Fig. 9. This concentration gradient profile closely resembles curves representing the solution of Fick's law for a sphere.[7] It should be possible to estimate the diffusivity of lead, using this profile, if the thermal history of the particle is known.

In this Laboratory, the matrix chosen for diffusion studies is the molten CaO-Al_2O_3-SiO_2 ternary. Experimentally, this system is very desirable since it is essentially invariant to very high-temperature, high-vacuum conditions; that is, its components are not very volatile compared with sodium- or potassium-containing silicate glasses. Since the calcium feldspars are a very common mineral, this ternary is representative of soils which might be involved in fallout formation. Many of the diffusion studies have been made using the eutectic composition of this ternary, sample E. The composition of the glasses was varied holding the ratio of CaO to Al_2O_3 constant. These samples correspond closely to those in the equilibration studies.

METHODS

Two methods were employed in the diffusion studies. One, which is called the plane-source technique,[8] involves loading platinum capillary crucibles (0.25 in. by 0.0785 in. ID, 0.10 in. OD) with a silicate matrix. The capillary is placed in a furnace and the matrix is melted. After removal from the furnace, the surface of the matrix is overlaid with a small amount of powdered glass, of composition identical to the silicate matrix except that it contains 0.05 to 3 mole-% of the radioisotopically tagged element being studied. The capillary is returned to the furnace and

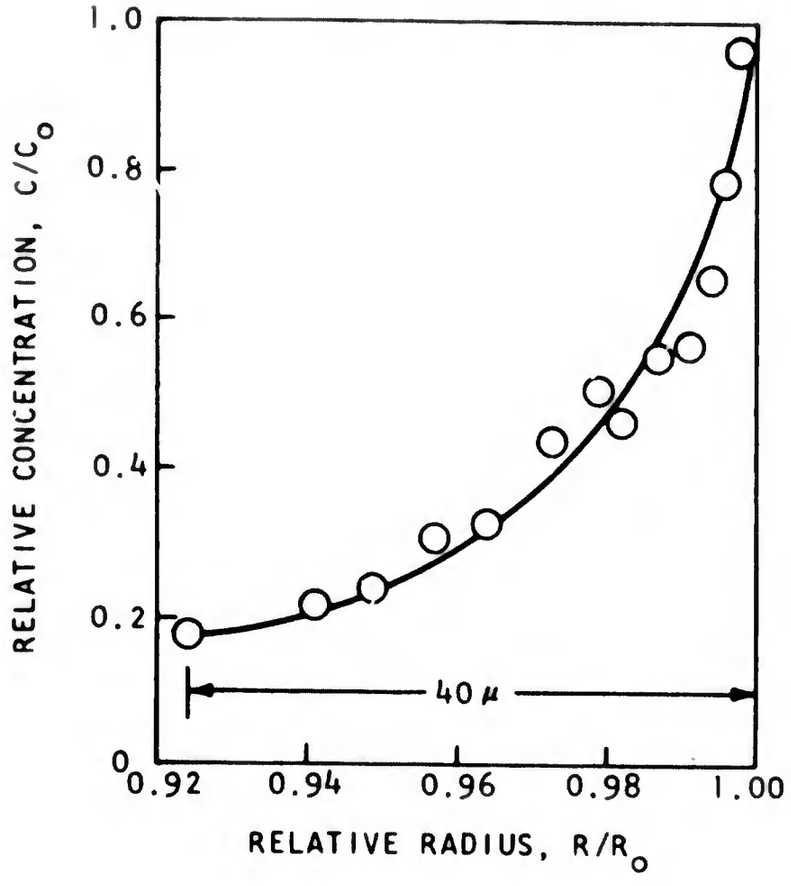

Fig. 9--Concentration gradient of lead in a fallout particle

maintained at a constant temperature for a known period. After the sample is removed from the furnace, the platinum may be removed, or retained in some cases. Then the sample is sectioned by grinding with emery paper and gamma-analyzed after measuring the length, or weight loss, of the sample. The grinding is repeated until most of the radioactivity is lost. Using the solution of Fick's law for a semi-infinite slab as a model,[8] the diffusivity is calculated from the equation

$$d \log_e C/d(X^2) = - 1/4Dt \quad , \qquad (1)$$

where C is concentration (cpm cm^{-3}), X is penetration distance (cm), t is time (sec), and D is the diffusivity (cm^2 sec^{-1}).

It is necessary to avoid bubbling of the matrix during diffusion runs. The formation of bubbles is minimized by prior melting and outgassing of the matrix at high temperatures and, in some cases, by adding 1/2% Sb_2O_3 to the glass as a fining agent.

A second method, which is called the vaporization technique, involves loss of the radionuclide from a molten, spheroidal particle in a high vacuum. In this technique, the matrix, which has been homogeneously doped with about 1% radionuclide, is melted onto a platinum-rhodium ring. The ring, made with 0.020 in. wire, has an inside diameter of roughly 0.065 in. Samples are simultaneously held and heated by the ring, which is a resistance element having a platinum-rhodium power lead connected to each side symetrically. These power leads are supported by high-vacuum lead-throughs in the removable base plate of a copper vacuum jacket. A Pt-Pt/10% Rh thermocouple made with 0.010 in. wire, spot welded to the ring, monitors the temperature. The thermocouple leads are brought through the base plate by lead-throughs to a potentiometer. The base plate is set off from the vacuum jacket by an O-ring and is clamped in place. The jacket is pumped by a high vacuum system, and pumped and cooled by liquid nitrogen surrounding part of the jacket. A sketch of the apparatus is shown in Fig. 10.

The loss of radionuclide, after heating the ring with the sample for a known length of time at a fixed temperature, is measured by removing the base plate with the sample in place and inverting the structure in a jig so that the sample, near the crystal of the gamma-analyzer, can be accurately counted. Following gamma analysis, the structure is returned to the vacuum jacket and another vaporization is carried out either at the same or at a different temperature. This process is repeated until, for practical purposes, the radionuclide is exhausted.

The model for the vaporization technique is the solution of Fick's law for a sphere.[7] It can be shown that after n isothermal diffusion

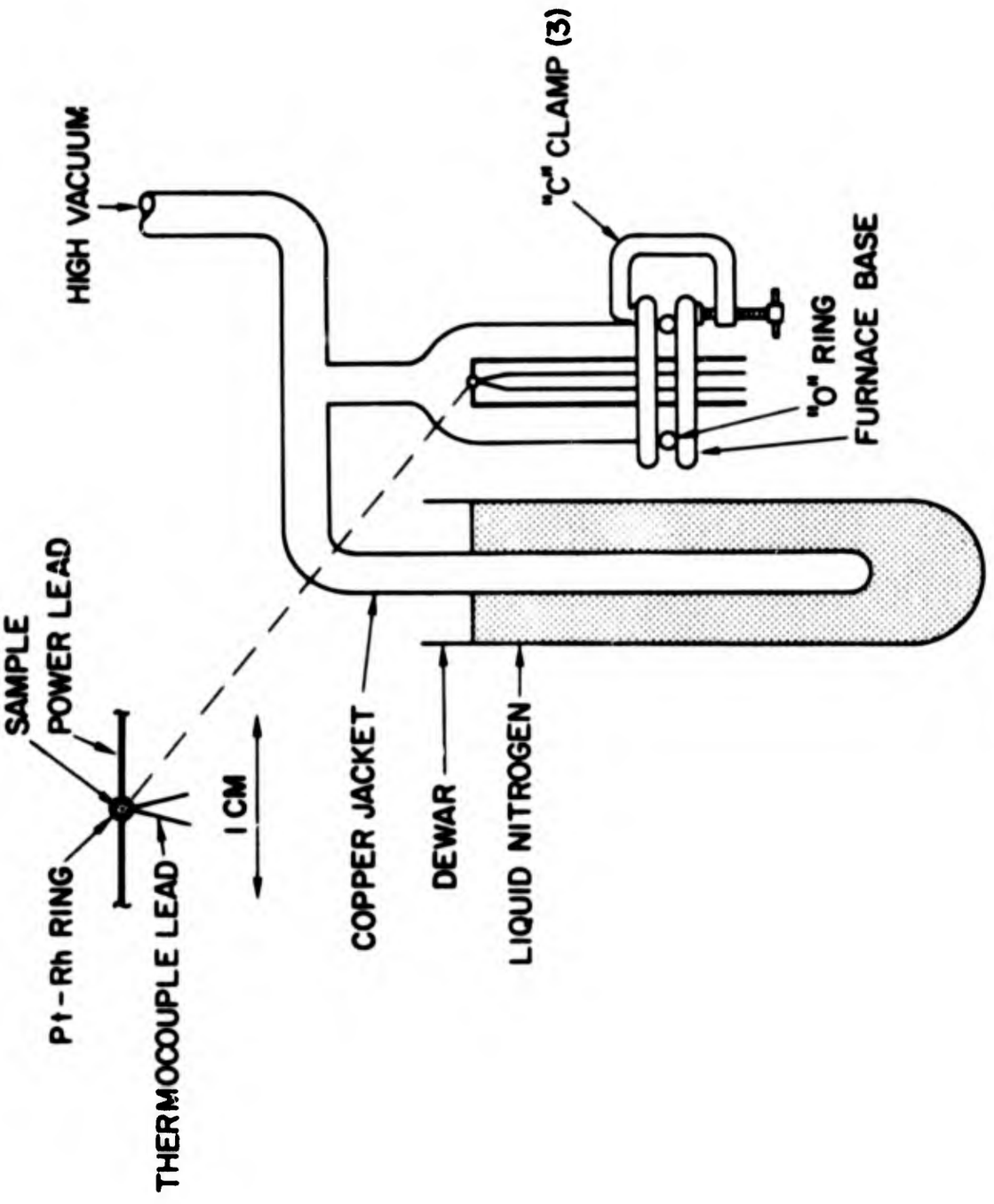

Fig. 10--Apparatus used in the vaporization technique

measurements on a particular sample

$$\frac{\bar{C}_n}{C_o} = \frac{6}{\pi^2} \sum_{a=1}^{\infty} \frac{1}{a^2} \exp\left[-\left(\frac{a\pi}{R}\right)^2 \sum_{b=1}^{n} D_b \Delta t_b\right] , \qquad (2)$$

where $\bar{C}$ is average concentration (cpm), C_o is initial concentration (cpm), D is diffusivity ($cm^2\ sec^{-1}$), t is time (sec), R is radius (cm), and $\Delta t_b = t_b - t_{b-1}$. When $\bar{C}/C_o \lesssim 0.3$, Eq. (3) can be approximated, with little error, by

$$\frac{\bar{C}_n}{C_o} \cong \frac{6}{\pi^2} \exp\left[-\left(\frac{\pi}{R}\right)^2 \sum_{b=1}^{n} D_b \Delta t_b\right] . \qquad (3)$$

The average-concentration ratios for successive measurements are then given by

$$\bar{C}_n / \bar{C}_{n-1} \cong \exp\left(-\pi^2 D_n \Delta t_n / R^2\right) . \qquad (4)$$

In practice, the samples are initially vaporized until $\bar{C}_1/C_o \cong 0.3$ prior to carrying out a set of measurements. This step, besides fulfilling a mathematical requirement, provides a preliminary, high-temperature outgassing of the sample.

A natural extension of this approach is to successively measure the diffusivity in the sample at different temperatures; in this way, the activation energy, E^*, as well as diffusivities, may be obtained for a single sample. An example of the loss of radioactive cesium from a molten glass at successively different temperatures is shown in Fig. 11.

The vaporization technique has been used because of its simplicity and rapidity when compared with the plane-source technique. The ability to carry out many diffusion studies on a single sample is, we think, novel.

The condition of diffusion limitation is necessary for the applicability of the vaporization technique. Theoretically, when

$$\bar{C}_1/C_o \lesssim 0.3 ,$$

the rate loss observed using this technique should be first-order:

$$dc/dt = -kt \quad (k > 0) . \qquad (5)$$

Experimentally, first-order dependence is found. However, a surface-limited, Henry's law–Langmuir vaporization would also exhibit first-order

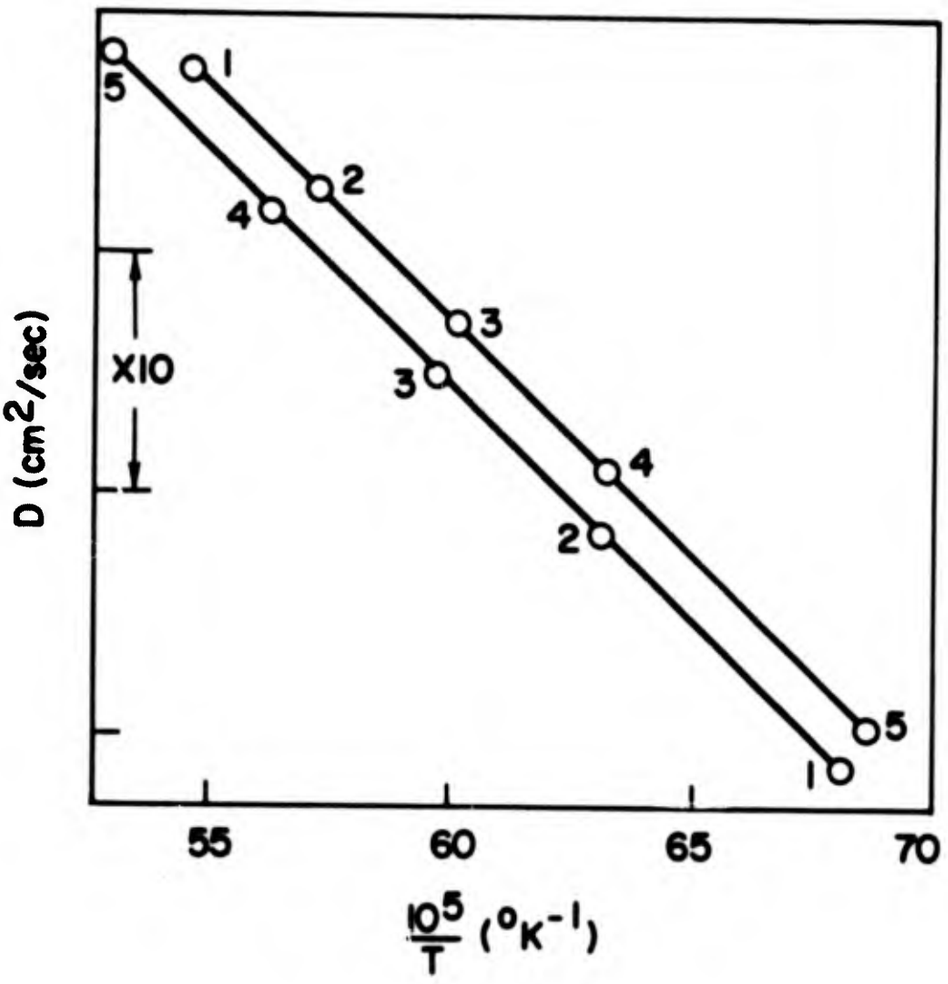

Fig. 11--Temperature dependence of diffusion coefficient of radioactive Cs in two $CaO-Al_2O_3-SiO_2$ samples of identical composition but with different radii (points are numbered according to order of experiments)

kinetics. Whether the data result from diffusion control or from surface control could be decided if the sample volume-to-surface area ratios could be greatly changed. Unfortunately, the technique does not allow such changes. Therefore, to find evidence of diffusion control, samples which had lost roughly 80% of C_o were sectioned in order to look for concentration gradients. In these experiments, tellurium showed no diffusion profile, cesium showed a diffusion profile only in the high-temperature experiment, and antimony showed diffusion profiles in both cases. It is believed that the evaporation rates of these elements were limited by diffusion. That is, enough information is now available to permit comparison of the data from vaporization techniques with data from plane-source techniques wherein diffusivities are determined from diffusion profiles. It is found that for cesium, tellurium, antimony, and molybdenum diffusing in matrix E, the two methods give identical results within reasonable uncertainties when the vaporization-technique data are treated as diffusivities. However, we feel the results obtained in the study of diffusion of antimony in silicates seem more reliable than the results for the other elements. It was therefore decided to investigate, by the vaporization technique, the effect of matrix composition on the transport of antimony, as an indication of the influence of this variable.

RESULTS

It has been the purpose of this part of the program to follow the thermal histories of several species diffusing in the same matrix and at least one species diffusing in different matrices. First, the data for several species in matrix E will be discussed. The over-all uncertainties in D and E^* are about 57% for D and about 10 kcal $mole^{-1}$ for E^*. The results for four species diffusing in E are shown in Figs. 12, 13, 14, and 15, and are summarized by

$$\log_{10} D = A - (B/T) \qquad (D \approx cm^2\ sec^{-1},\ T \approx {}^{o}K)\ , \tag{6}$$

where the coefficient A is related to the activation entropy, ΔS^*, and the coefficient B is related to the experimental activation energy, E^*. Experimental values of A and B are presented in Table 2.

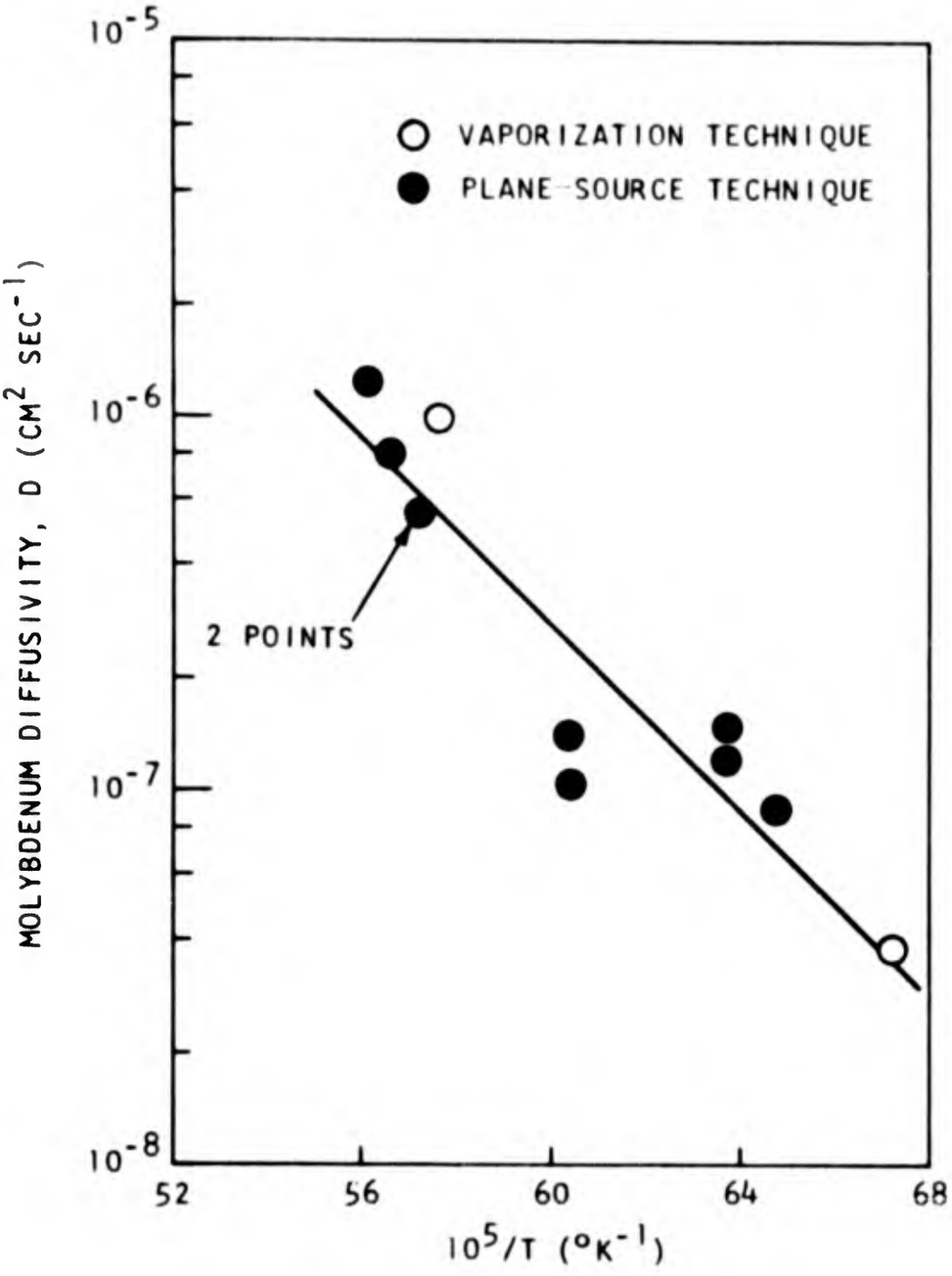

Fig. 12--Diffusivity of radioactive molybdenum in matrix E as a function of reciprocal temperature

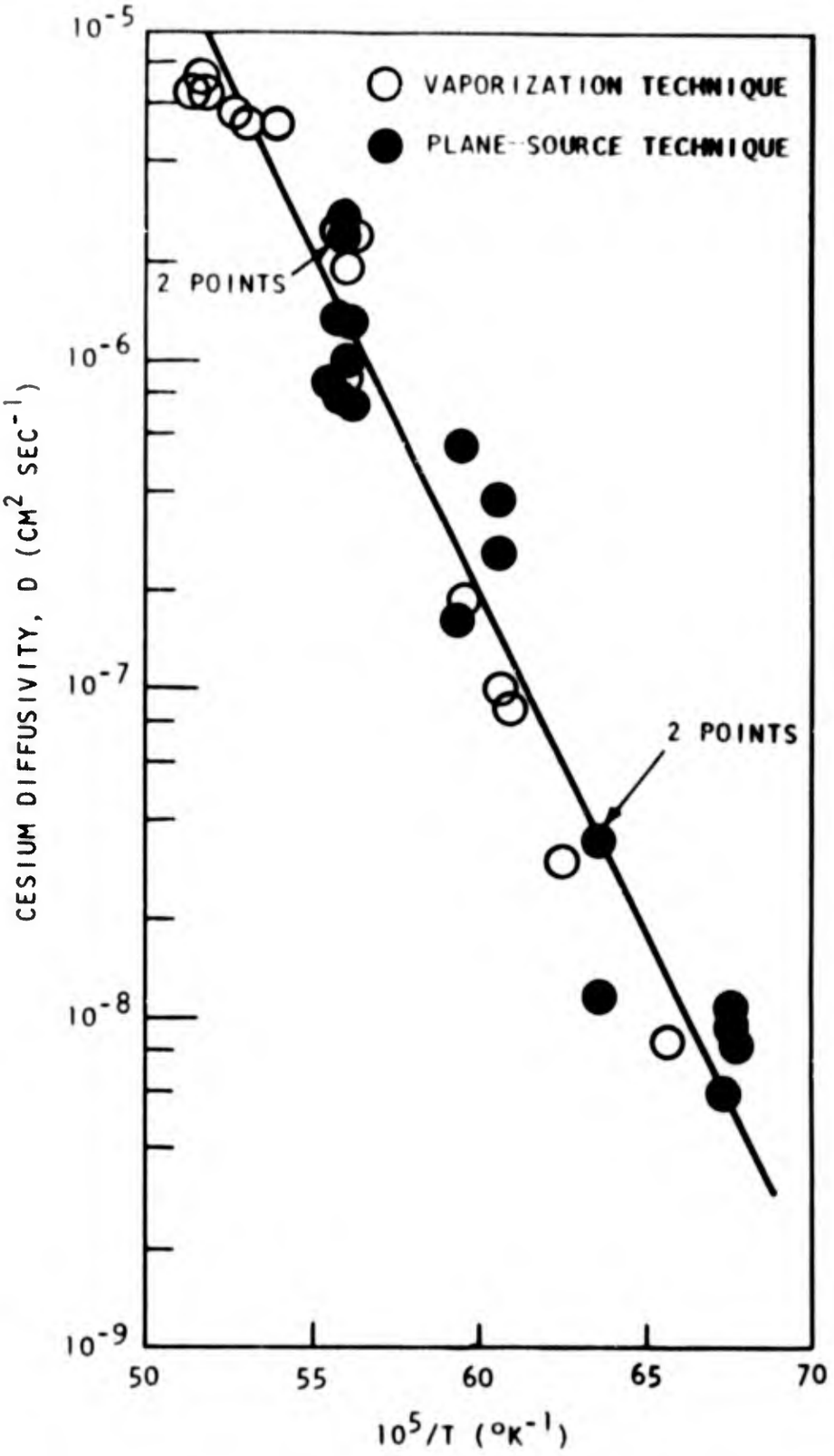

Fig. 13--Diffusivity of radioactive cesium in matrix E as a function of reciprocal temperature

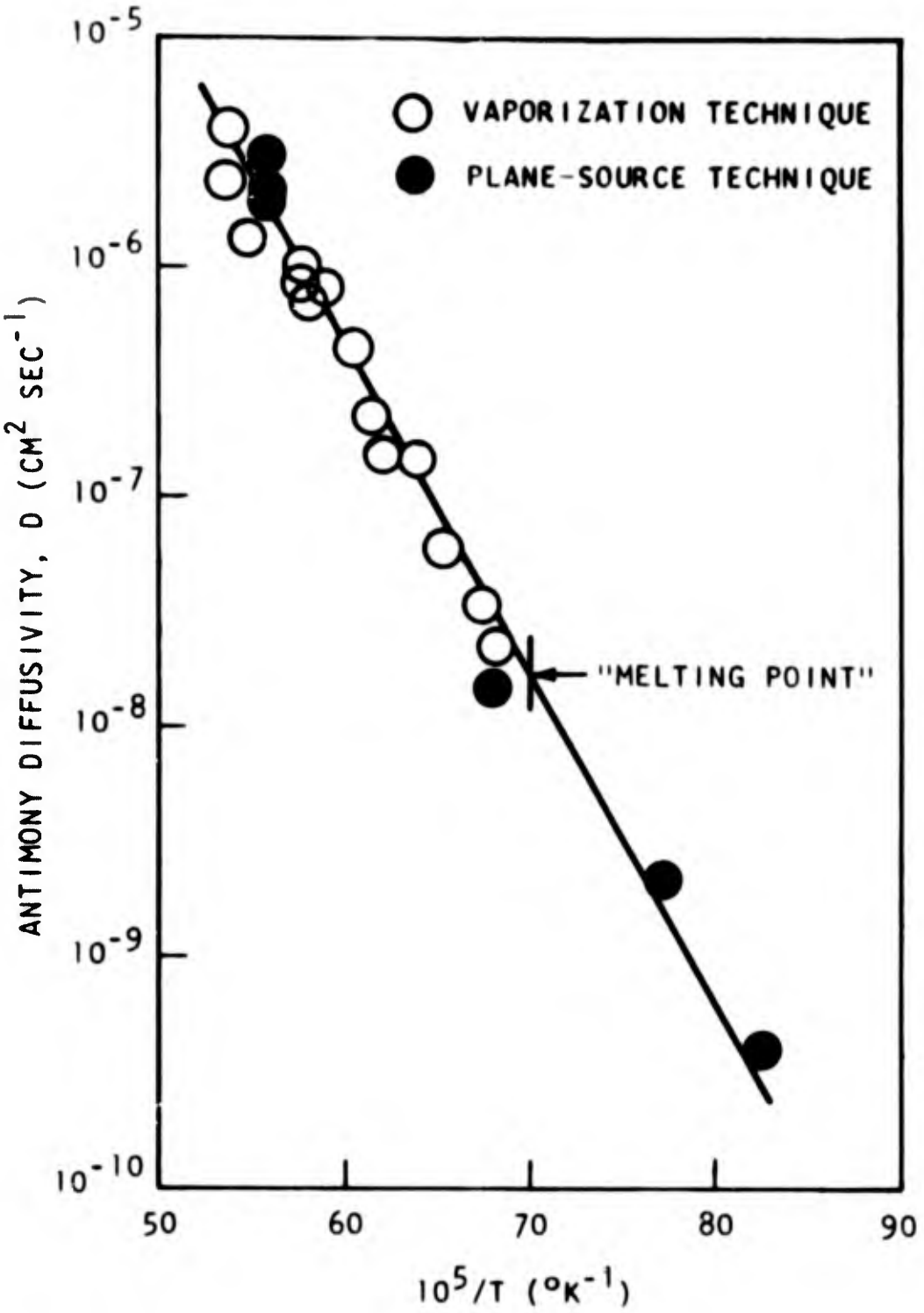

Fig. 14--Diffusivity of radioactive antimony in matrix E as a function of reciprocal temperature

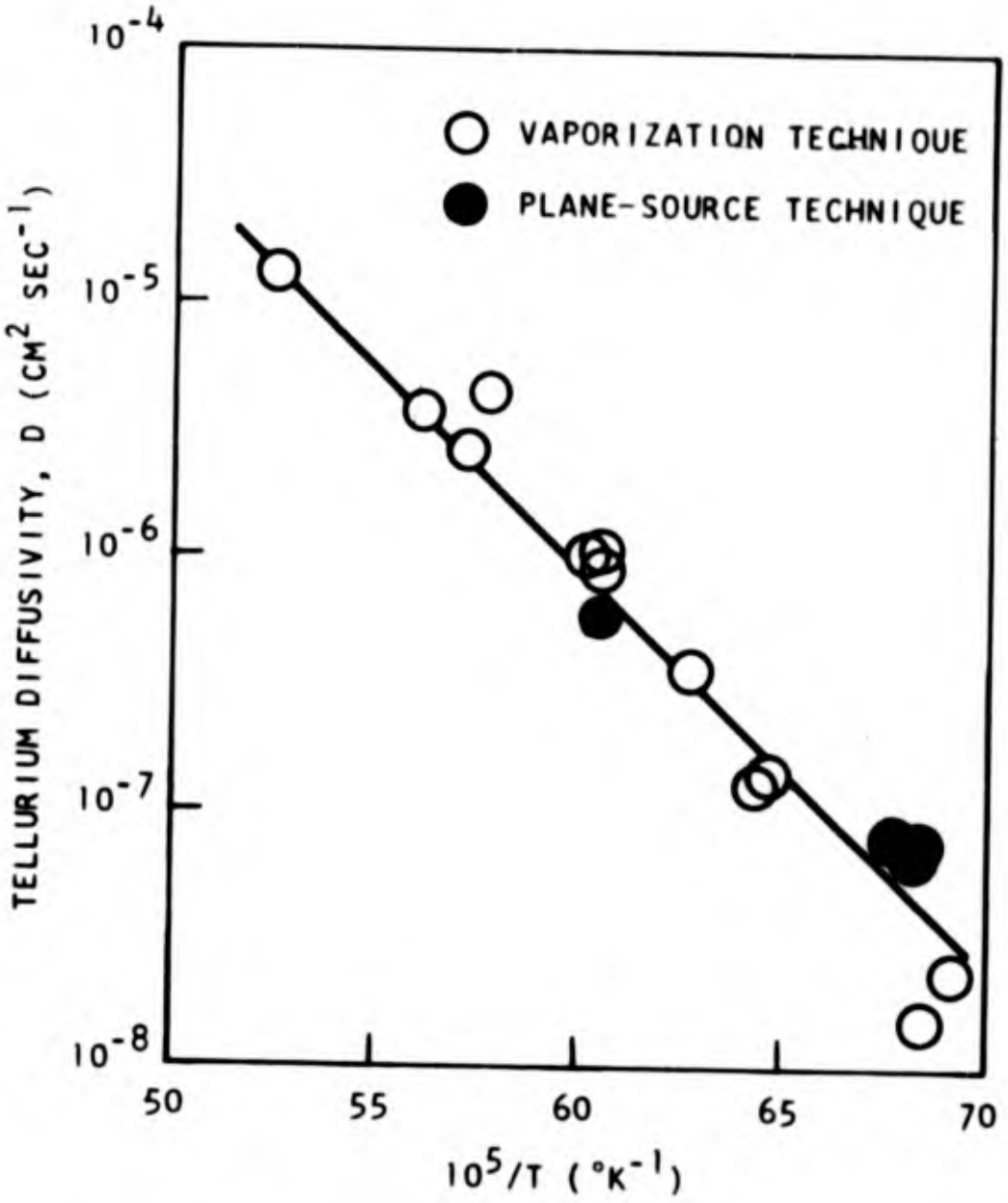

Fig. 15--Diffusivity of radioactive tellurium in matrix E as a function of reciprocal temperature

Table 2

EXPERIMENTAL VALUES OF A AND B

Species	A	B × 10^{-3}
Cs	5.57	20.5
Te	3.30	15.6
Sb	2.10	14.1
Mo	0.94	12.5

One would expect that there should be some correlation between the size of a diffusing species and the diffusivity. Ralkova[10] has demonstrated the linear relation between $\log_{10} D$ and reciprocal ionic radius, r^{-1}, for four alkali metal ions diffusing in a glass at 350°C. He has also compared the diffusion of Cs^{+} with Sr^{++} at various temperatures and has concluded that the importance of valency in diffusion decreases with increasing temperature. In the present work, it seems certain that cesium diffuses as Cs^{+}, but the ionic nature of tellurium, antimony, and molybdenum is uncertain. If it is assumed that these species diffuse as Te^{+4}, Sb^{+3}, and Mo^{+6}, a correlation can be found between the activation energy, E^{*}, and the reciprocal ionic radius, r^{-1}. There are data for calcium diffusion in a similar matrix.[11] Calcium is considered to diffuse as Ca^{+2} in silicates. The E^{*} to r^{-1} correlation is shown in Fig. 16, where the Ca^{+2} data have been included for comparison. It is emphasized that an E^{*} to r^{-1} correlation can be demonstrated, but it is tenuous because of the assumptions involved. It was also noted that there is a correlation between E^{*} and atomic number for cesium, tellurium, antimony, and molybdenum.

Viscosity isotherms have been reported[12] for the $CaO\text{-}Al_2O_3\text{-}SiO_2$ ternary at high temperatures. Using this information, and the diffusivities for cesium, tellurium, antimony, molybdenum, and calcium, effective radii can be calculated for these species using the Stokes-Einstein equation

$$D = kT/6\pi\eta r \quad , \tag{7}$$

where D is diffusivity ($cm^2\ sec^{-1}$), k is Boltzmann's constant ($erg\ {}^{\circ}K^{-1}$), T is temperature (°K), r is radius (cm), and η is viscosity (poise). Calculations were made at several temperatures. In all cases, the calculated radii were very small (e.g., 0.05 Å). Evidently the Stokes-Einstein equation does not apply in this case. This result is in agreement with the findings of King and Koros.[13]

Results from the study of diffusion of several radionuclides in the same molten silicate, E, reflect the complexity of these systems. One of

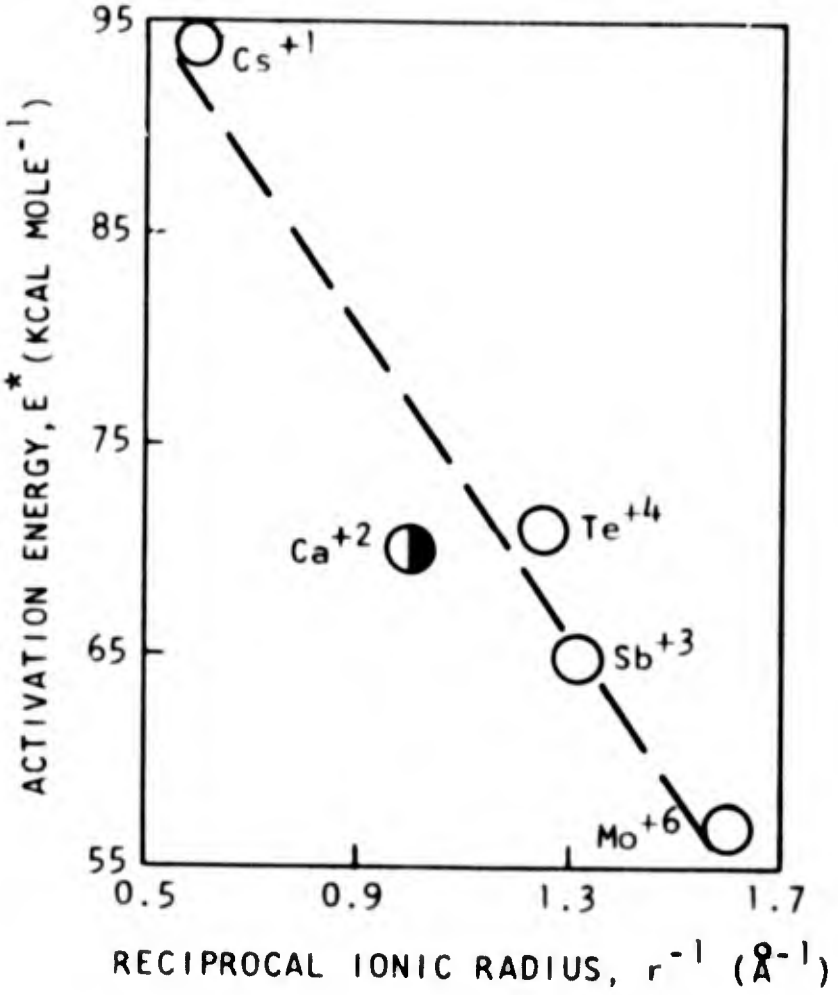

Fig. 16--Correlation of activation energy for diffusion with reciprocal ionic radius for species diffusing in molten CaO-Al_2O_3-SiO_2 of near eutectic composition (value for calcium obtained from Ref. 11)

the aims of these studies would be the prediction of the diffusivity of some species in a particular silicate. However, it seems that such a prediction, although possible, would be very uncertain at this point.

Diffusion of antimony was chosen for a study of the matrix-composition dependence of diffusion. The vaporization technique was employed. Powdered glasses were doped with 1% Sb_2O_3, melted, powdered, and remelted. The samples were then activated in the General Atomic TRIGA reactor to yield 60-day Sb^{124}. The matrix composition was varied, keeping the CaO to Al_2O_3 ratio constant. Sample densities were calculated from the equation[14]

$$\frac{1}{\rho} = \sum_i (x_i v_i) \quad , \tag{8}$$

where x_i is the weight fraction of component i and v_i is the specific volume of this component. The density and sample weight were used to calculate the radius of the spheroidal diffusion samples. Literature values[15] show that the densities of common high-temperature substances change little from 25° to 1700°C, the volumetric expansion being a few percent. Therefore the sample radii were uncorrected for thermal expansion changes. The following table summarizes the matrix compositions and densities used.

Table 3

SUMMARY OF MATRIX COMPOSITIONS AND DENSITIES

Matrix	CaO (%)	SiO_2 (%)	Density (g cm^{-3})
A	33	34	2.9
B	28	45	2.8
BE	25	50	2.7
E	22	55	2.7
EC	19	59	2.6
C	17	63	2.6

Since the CaO/Al_2O_3 ratio was constant for the six samples, the equivalent SiO_2 content is used for comparing diffusion data with composition. Table 4 summarizes the data according to Eq. (6). The over-all uncertainties are ±10 kcal $mole^{-1}$ for E^* and about 50% for D. It is seen from Table 4 that the composition of the $CaO\text{-}Al_2O_3\text{-}SiO_2$ matrix strongly affects the constants A and B. The over-all effect of composition on the

antimony diffusivity is shown in Fig. 17, where the composition dependence is given for three temperatures, 1587°, 1727°, and 1866°K. It is clear that antimony diffuses less readily in high-silica matrices and that this dependence is diminished as the temperature is decreased or the silica content is decreased. Reported viscosity data[12] show that the viscosity of this matrix increases monotonically with increasing SiO_2 content. Thus, the diffusivity decrease with increasing SiO_2 content is not unexpected. However, this evidently occurs only in the silica-rich region, the diffusivity remaining approximately constant in the low-silica region. Johnson, Bristow, and Blau[16] report a linear, increasing relationship between log D and mole-% Na for diffusion of Na in Na_2O-SiO_2 glasses at 1000°K and Na concentrations ranging from roughly 4 to 13 mole-%.

Table 4

COMPARISON OF DIFFUSION DATA WITH COMPOSITION

SiO_2 (Equiv. %)	A	B × 10^{-3}	No. Points	Temp. Range (°K)
34	7.39	22.3	5	1587 - 1748
45	8.90	24.5	8	1613 - 1779
50	4.72	17.5	4	1672 - 1824
55	2.10	14.1	25	1215 - 1866
59	4.55	19.2	4	1739 - 1852
63	9.32	27.8	7	1739 - 1866

Referring to Table 4, the correlation between A and B is evident. The dependence of the activation energy on composition is shown in Fig. 18. It is clear that E^* passes through a minimum at the eutectic composition of the CaO-Al_2O_3-SiO_2 ternary. It is felt that this is a true minimum and not a discontinuity, since the latter would imply phase segregation of the sample, which has not occurred for E in these experiments. Phase segregation was evident only in two samples of 63 equiv. -% SiO_2 at the lowest temperatures, and the results were discarded. The curve in Fig. 18 bears a striking resemblance to the activation energy for d-c conduction in a series of $Na_2O \cdot xAl_2O_3 \cdot 2(4-x)SiO_2$ glasses,[9] where a minimum in E^* occurs at x = 1. This minimum in E^* for the sodium glasses is explained[9] by stating that at x = 1 all the oxygen atoms in the matrix are in a bridging position and the shell of oxygen atoms is expanded around the sodium atoms, thus lowering the d-c resistivity. For the calcium-feldspar composition glasses, there is at least one case reported[17]

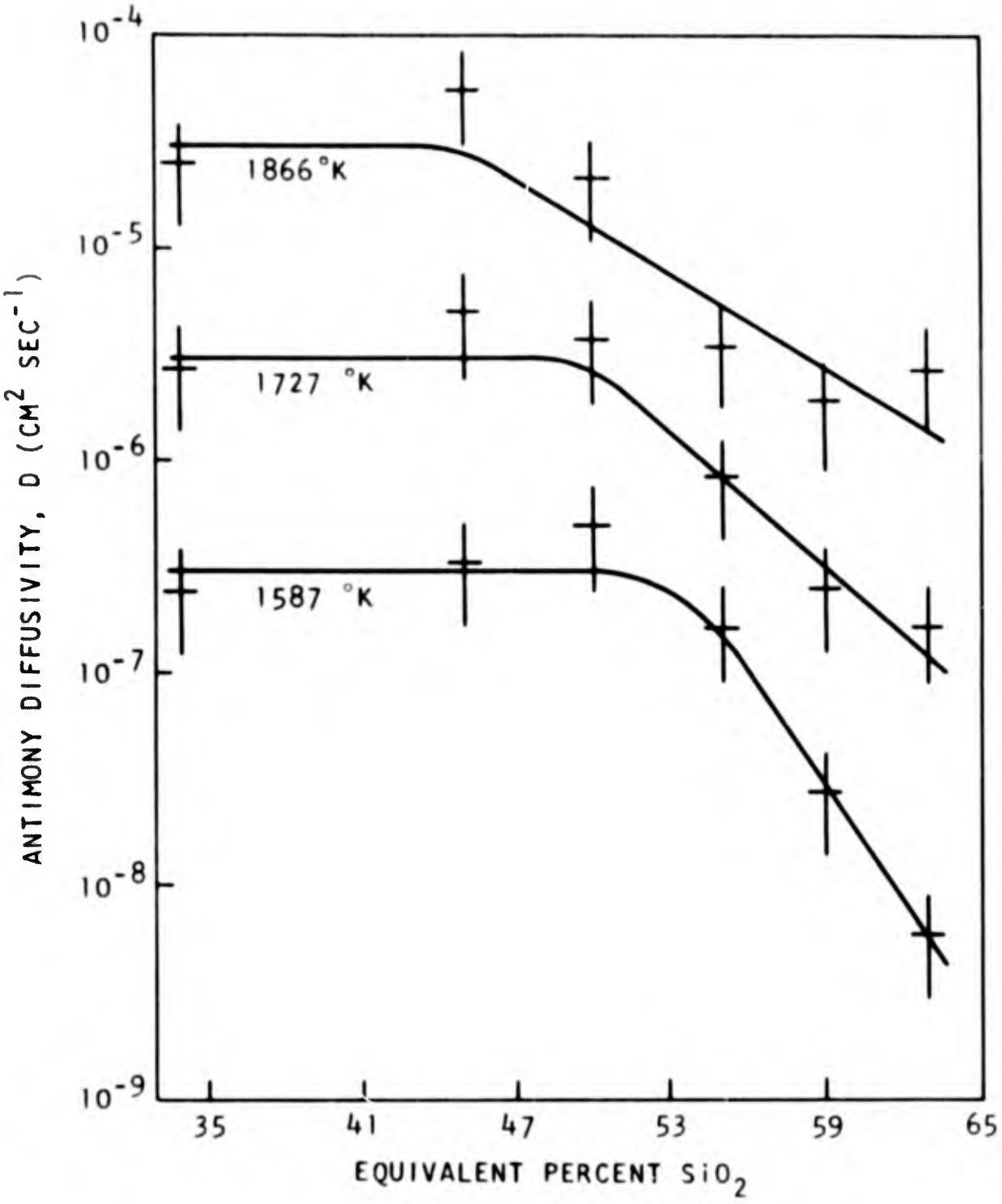

Fig. 17--Composition dependence of radioactive antimony diffusion in molten CaO-Al_2O_3-SiO_2 matrices at three temperatures

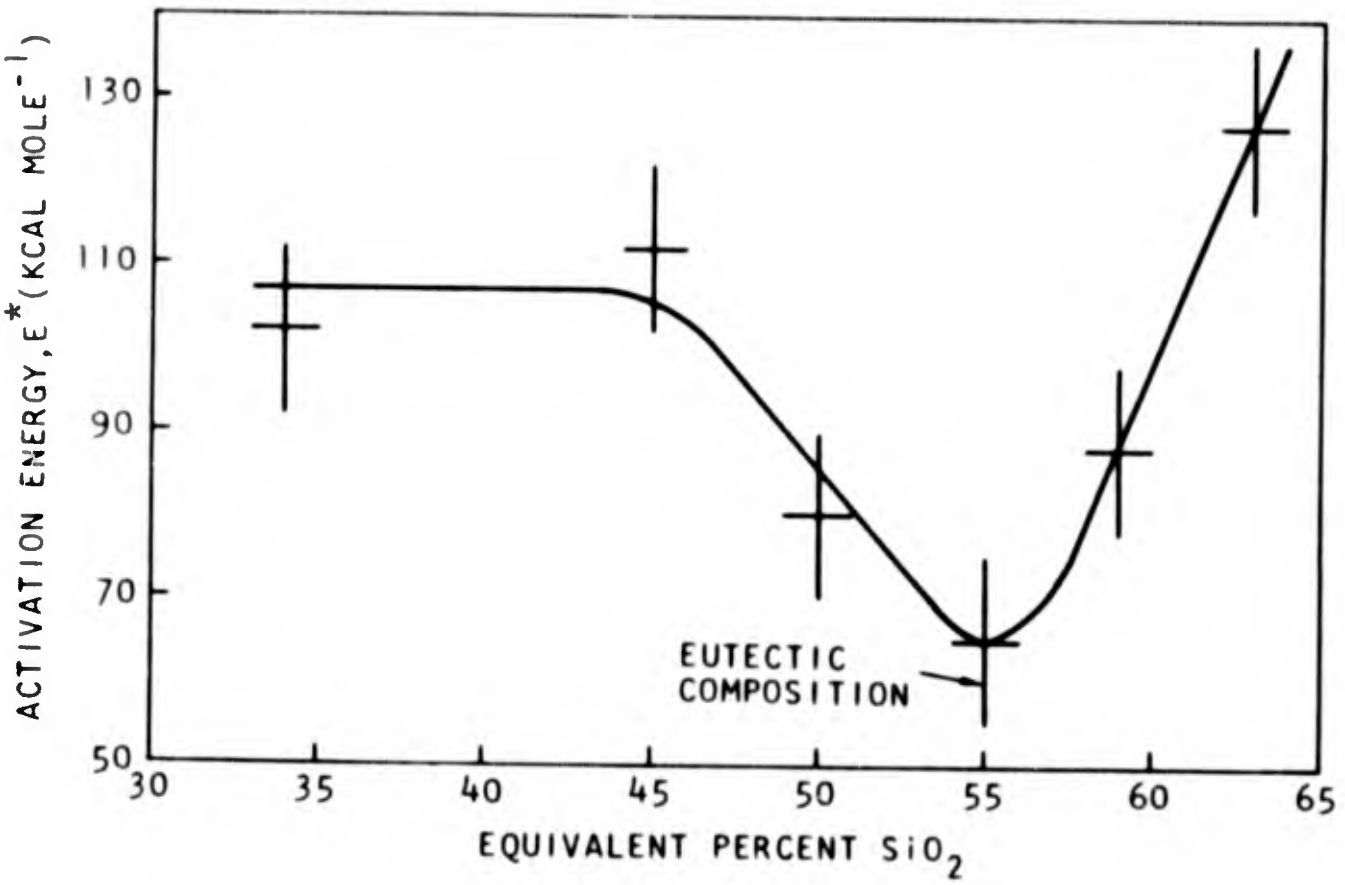

Fig. 18--Composition dependence of activation energy, E^*, for diffusion of radioactive antimony in molten $CaO-Al_2O_3-SiO_2$ glasses

where E^* has a minimum value. At present, there seems to be no simple explanation for the compositional dependence of E^* shown in Fig. 18. It would seem that the structure of the eutectic melt, compared to the other reported melts, is such that interstitial transport of antimony is least difficult. The entropy term, A, has as strong a composition dependence as has E^* and also exhibits a minimum at E.

As in the case of cesium, tellurium, antimony, molybdenum, and calcium in E, calculations using the diffusion and viscosity data[12] and the Stokes-Einstein relation result in very small effective radii.

In summary, diffusion of four radionuclides in the same calcium-aluminum-silicate glass has been studied over a wide temperature range by two techniques. The diffusion of radioactive antimony has been studied, over shorter temperature intervals, as a function of composition of the glass. The uncertainties for the diffusivity, D, and for the activation energy, E^*, have been derived. These data should prove useful in formulating kinetic descriptions of fallout models.

IV. MASS SPECTROMETRIC STUDIES OF THE ALKALINE EARTH METAL OXIDES

We have, since the last report, added barium, calcium, and magnesium oxides to the studies of alkaline earth metal oxide vaporization reported previously. These studies, which were initiated on Office of Civil Defense funds, have been made with the purpose of learning more about fission product oxides and soil constituents. The result will only be summarized here, since a paper on these studies will be submitted for publication soon. These studies differ in two major ways from studies made on these systems by other workers. First, our studies were made using an iridium Knudsen cell, which allows attainment of neutral evaporating conditions and no cell-sample interaction. That is, the total oxygen evaporating from the cell can be closely related to the total metal evaporating and the oxide studied is at unit activity. Second, when appropriate, studies of these vaporizations have also been made feeding oxygen into the cell. The oxygen feed system is particularly valuable in the case of BaO vaporization, where the vaporizing species O, O_2, and Ba were not observable under neutral conditions and the species Ba_2O was quite apparent. To evaluate the thermodynamics associated with this last species, any one of the three species O, O_2, or Ba must be observed also.

To summarize these results, the vapor pressures of the species observed under neutral vaporizing conditions at 2000°K are presented in Table 5 as calculated using silver calibrations according to Inghram and Drowart[18] and estimated cross sections, according to Otvos and Stevenson.[19] Heats of vaporization of MO and M_2O_2, and heats of the reaction $MO(s) \rightarrow M(g) + O$ and $2MO(s) \rightarrow M_2O(g) + O$ are presented in Table 6.

Table 5

VAPOR PRESSURES OF SPECIES OVER ALKALINE EARTH METAL OXIDES AT 2000°K UNDER NEUTRAL EVAPORATING CONDITIONS
(In atm)

Species	MO	M	O_2	O	M_2O_2	M_2O
Mg	(a)	7.49×10^{-6}	2.79×10^{-6}	1.19×10^{-6}	---	---
Ca	1.14×10^{-8}	5.27×10^{-7}	2.42×10^{-7}	1.40×10^{-7}	1.05×10^{-10}	2.68×10^{-10}
Sr	3.06×10^{-7}	5.86×10^{-6}	1.39×10^{-6}	9.25×10^{-7}	4.57×10^{-9}	7.91×10^{-10}
Ba	2.10×10^{-4}	---	---	---	4.95×10^{-6}	Pending

[a] At 2272°K MgO^+ was less than 1/18,000 of Mg^+.

Table 6

HEATS OF VAPORIZATION FOR CERTAIN SPECIES FROM ALKALINE EARTH METAL OXIDES AT 2000°K
(In kcal/mole)

Species	MO	M_2O_2	M+O	M_2O+O
Mg	---	---	211.7±9.6	---
Ca	144.2±5.5	150±13	240.1±6.4	318±6
Sr	118.2±3.1	135.2±5.5	206.6±7.1	282±8
Ba	96.1±1.1	107.2±3.3	---	227±11[a]

[a] $P_{M_2O} \cdot P_O^{1/2}$ at 2000°K = 1.43×10^{-10} $atm^{3/2}$.

V. MICROPROBE STUDIES

We have previously reported[1] some preliminary observations on an individual fallout particle with an electron microprobe. We have since made a somewhat more extensive study with the expressed purpose of further delineating the phenomena that occur during fallout formation--accretion of particles, diffusion within a particle, and absorption of elements into a particle.

Six fallout particles from an apparently relatively low yield tower shot have been sectioned. While these particles may not be statistically representative of all fallout particles, as they were selected because their outward appearance suggested the occurrence of accretion of particles, they certainly must reflect typical phenomena occurring during fallout formation.

To illustrate what can be done with an electron microprobe, Fig. 19a shows a composite "potassium picture" of one of the particles. It was obtained by measuring the potassium K_α fluorescence as a function of position on the face of the sectioned particle. The light spots indicate the presence of potassium--the lighter the region is, the higher the potassium content. The dark spots, then, are places where the potassium content is quite low. Potassium content can be low for two reasons: either there is no potassium on that portion of the face of the particle or there is no face of the particle in the portion under consideration--a void. Both of these situations occur for this particle--voids where bubbles were cut into, and no potassium where high silica phases were encountered, as shown in other microprobe studies. Figure 19b is a diagram labeling the different features in Fig. 19a--v stands for void and S for high silica areas as determined indepent of these figures with the microprobe. Figure 19c is a photograph of this particle and Fig. 19d is a dark field photograph (oblique lighting) of this same particle.

Let us consider the formation of this particle as suggested by this information:

1. The particle is spherical. This strongly indicates that the particle was at least partially molten at one time. This is supported by the nearly spherical bubble craters well distributed in the particle matrix.

2. The particle is not homogeneous, indicating slow condensed state diffusion and/or short heating times. While one does not rely

(a)

(b)

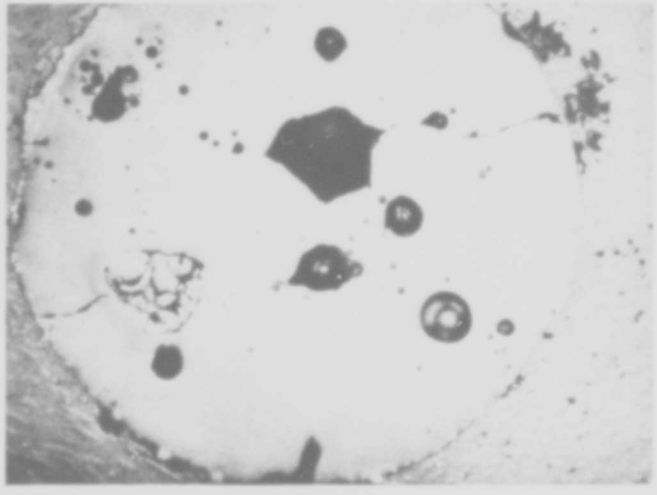

(c)

(d)

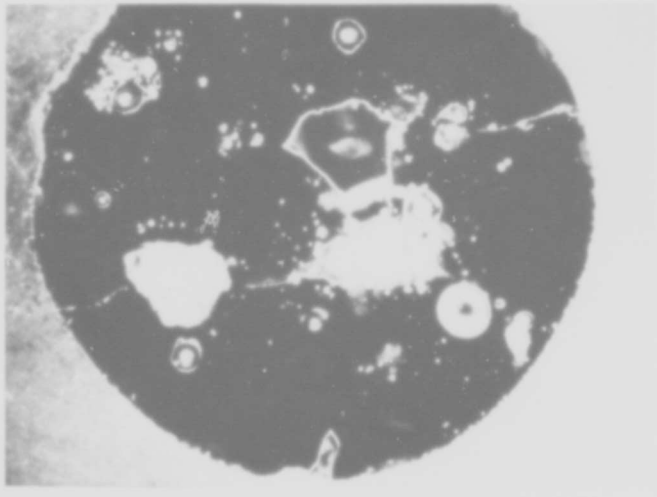

Fig. 19--Microprobe studies of a fallout particle: (a) composite K K_{α} microprobe intensity picture; (b) diagram of the particle; (c) photomicrograph of the particle; (d) dark field photomicrograph of the particle

strongly on the differences in shading in the high potassium areas to denote inhomogeneity, one certainly does recognize the near absence of potassium from the high silica areas. It is true, however, that one reason why the potassium may not have mixed with the silica phase is that the silica phase may not have been melted. However, there is strong evidence, in the heart-shaped phase and the phase near the hexagonal void, that some melting of silica did occur. For example, the heart-shaped phase extends well beyond the cracked region, as shown by the electron back scatter, Fe Kα, and Si Kα intensities shown in Figs. 20a, 20b, and 20c, respectively. A photomicrograph of this feature is shown in Fig. 20d. Back scatter intensities indicate differences in molecular weight of the matrix (light areas are high molecular weight). The outer portions of the heart-shaped phase thus do appear to have been well-mated to the main phase, suggesting melting even though it is probable that the center of this phase did not melt. Further inhomogeneities will be discussed later.

3. Inhomogeneities as indicated in Fig. 19 are a strong indication of the phenomenon of accretion. That is, either these silicate inclusions must have existed in a particle before it was brought into the nuclear cloud or the particle must be made up of many smaller particles--some of which, particularly those high in silica, can still be recognized as discrete particles. This latter explanation of the observations seems most plausible for silicate and other inclusions. Also, it would appear, because of the variable composition, that the silicates of this particle were generally not condensed from the vapor state.

4. Potassium content does not appear to be particularly high at the surface of the fallout particle, as had been anticipated for condensed state diffusion controlled fission product absorption. This suggests that potassium was not greatly vaporized from the particles which later accreted to make this droplet.

These points then would suggest (1) that soil particles were melted as they were sucked into the cloud, (2) that insufficient time was available at high temperature for these particles to lose their potassium (slow diffusion—short time demands little potassium movement), (3) that accretion of these soil particles of varying composition followed, leading to the fallout droplet, and (4) that cessation of accretion occurred when the viscosity and surface tension of the resulting silicate glass--the particles do appear to be mainly glassy--were sufficient that collisions were no longer effective in causing accretion.

Now let us look at other microprobe information to see if it supports and augments this description. Some of the simple findings involving potassium, silicon, and electron back-scatter intensities include a round high-potassium region near the surface of one of the particles, silica

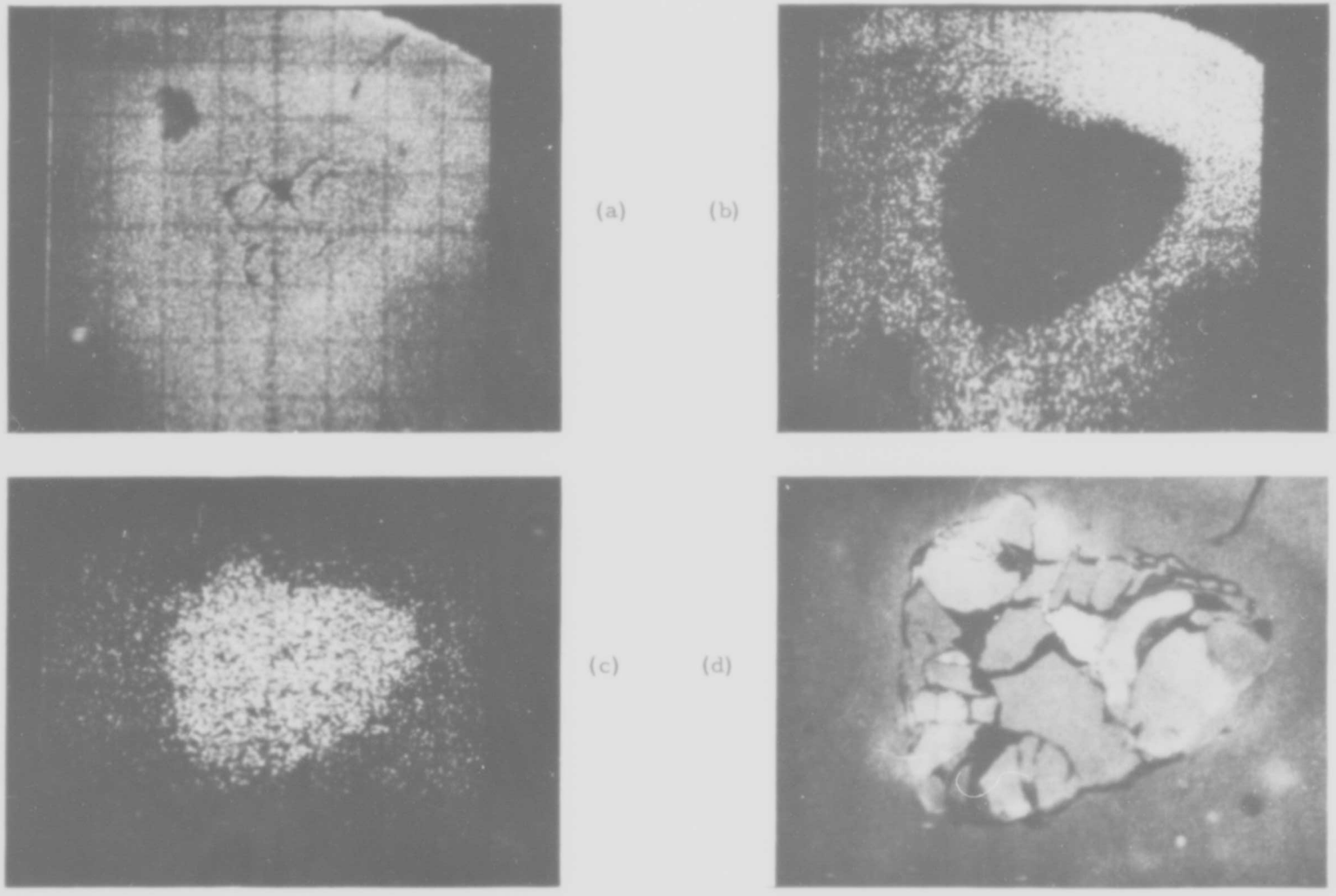

Fig. 20--Microprobe studies of a feature of the fallout particle: (a) electron back scatter intensity picture; (b) Fe K_{α} intensity picture; (c) Si K_{α} intensity picture; (d) photomicrograph

inclusions in all of the investigated particles, and bubble-like voids in all the particles. Surveying these particles for lead and iron, however, results in some new, rather remarkable information concerning nuclear cloud chemistry. While observations concerning these elements are similar for all of the particles, let us choose two other particles to help present this information.

One of these particles, pictures of which are shown in Figs. 21a and 21b, exhibits a bubble-marked face and two protuberances on opposite sides of the particle. Figures 21c, 21d, 21e, 21f, 21g, and 21h represent, respectively, electron back scatter, Si K_α, K K_αa, Fe K_α, Ti K_α, and Pb M_α intensities of one of the protuberances. At least three different density areas--dark areas represent low molecular weight, and vice versa--are suggested in Fig. 21c. They are the dark sharp-cornered central inclusion, the very light region more or less surrounding this inclusion and the curved boundary delineating the outside of the particle, and the rest of the face. The Si K_α intensities show that the central inclusion was silica. Considering this as an unmelted silica fragment would account for the sharp corners of this inclusion. The potassium K_α intensities indicate little potassium content in the silica phase, suggesting a high melting point for this phase. They also show some variation in the potassium content in the rest of the particle. Note particularly the region of relatively high potassium content where the light spots on the picture seem nearly continuous. The Fe K_α intensities demonstrate that the high potassium spot is low in iron but there are adjacent areas that are high in iron, particularly those bordering the central inclusion. The Ti K_α intensities are very interesting because they indicate highly segregated titanium which more or less borders the central inclusion on the outside edge. The most striking intensity picture, however, is that of Pb M_α. The lead is demonstrated in this figure to border both the inclusion and the outside of the particle. This picture strongly supports the accretion model by suggesting that the silica inclusion was coated with lead (from device parts) and then was incorporated into the molten fallout particle. It also supports a diffusion model, since PbO (or Pb?) apparently was condensed on the outside of particles and has not equilibrated with the condensed phase. It would appear, then, that the accretion of the silica particle was followed by accretion with another particle; the viscosity of the matrix at this time was high enough that the final particle could no longer spheroidize. Lead boundaries for this second particle seem apparent in Fig. 21h. The time of the accretion of the second particle, then, would seem to be after the particles were coated with lead but before the matrix material was viscous enough that the smaller particle's borders would not blend into those of the larger particle.

The protuberance at the other end of the first particle is suggested to be caused by accretion of a high-iron droplet with the fallout particle

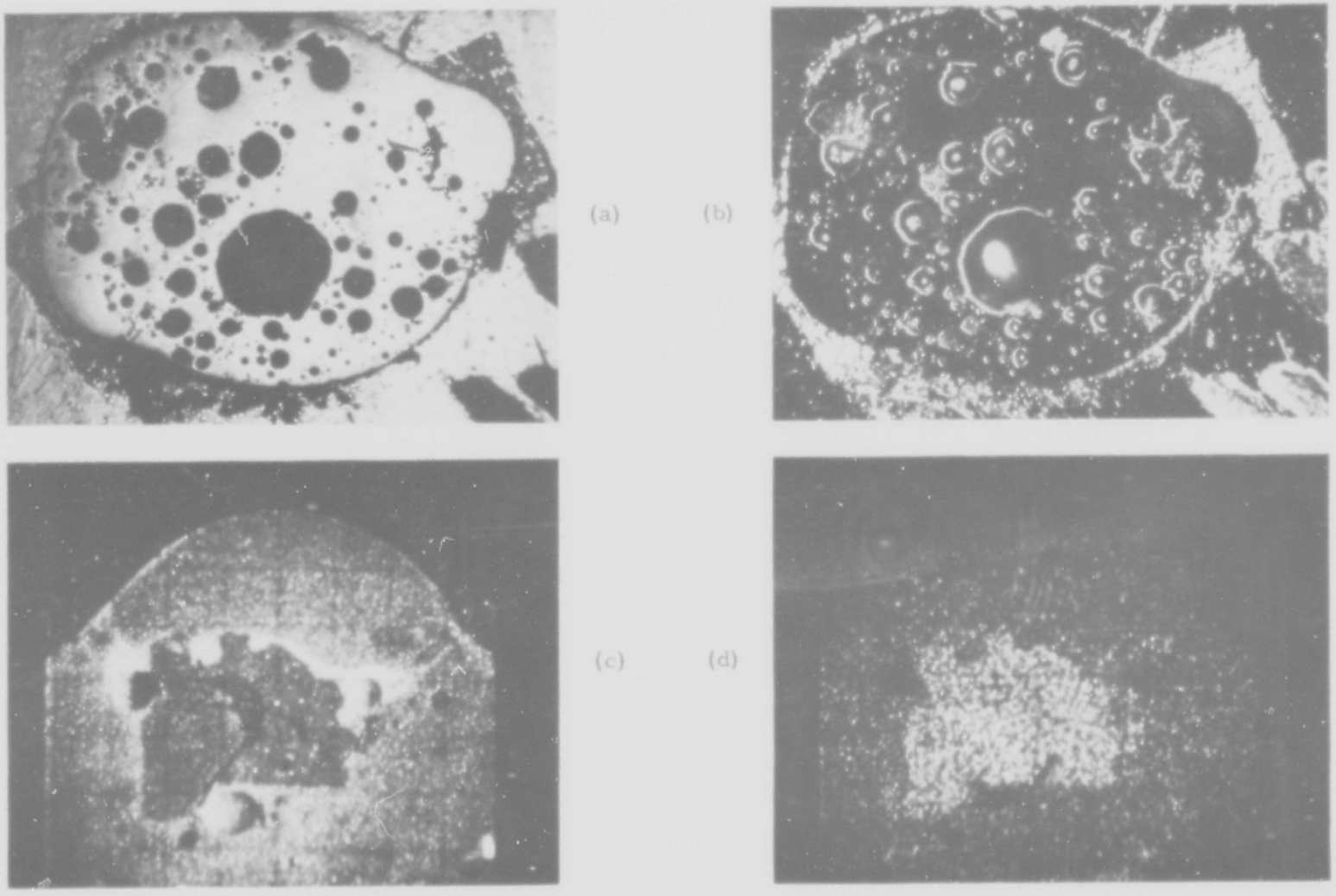

Fig. 21--Microprobe studies of another fallout particle: (a) light field photomicrograph; (b) dark field photomicrograph; (c) electron back scatter intensity picture; (d) Si K_α intensity picture of a feature

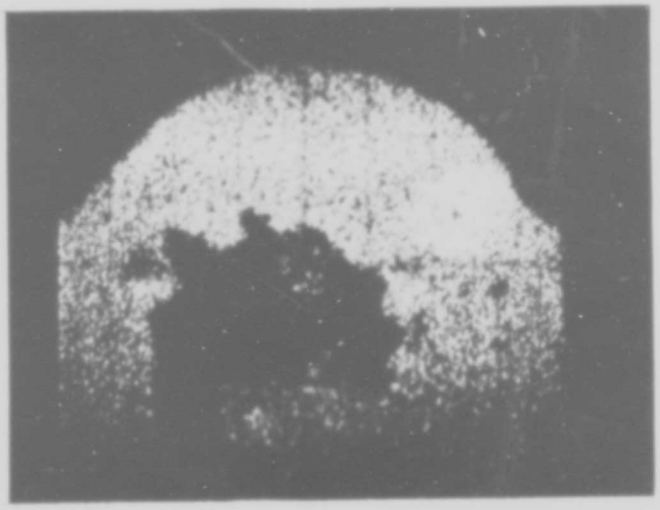

(e)

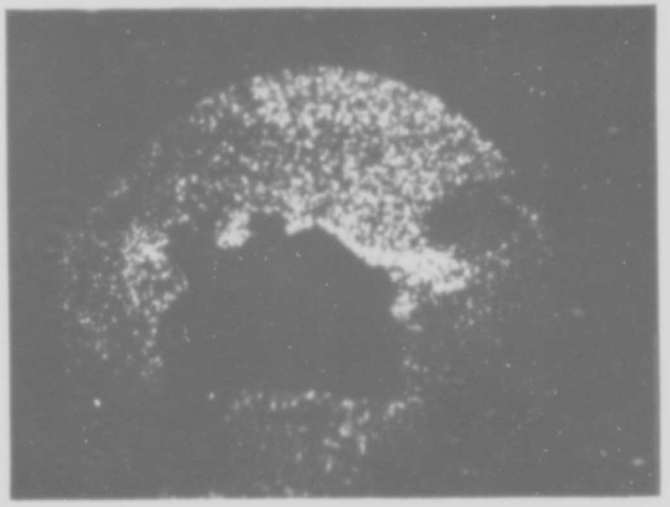

(f)

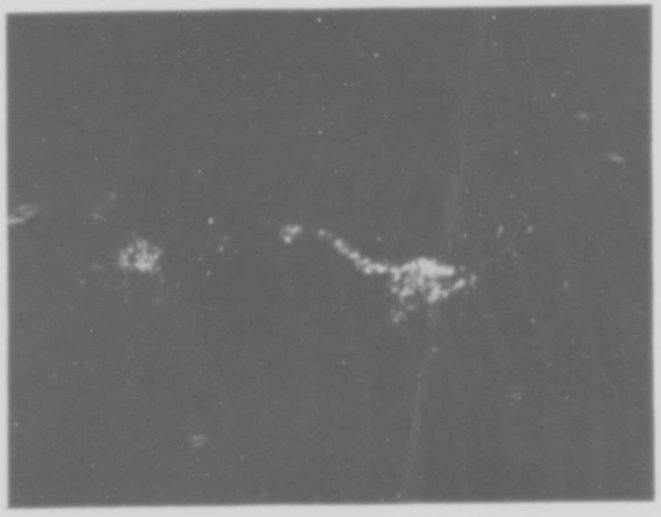

(g)

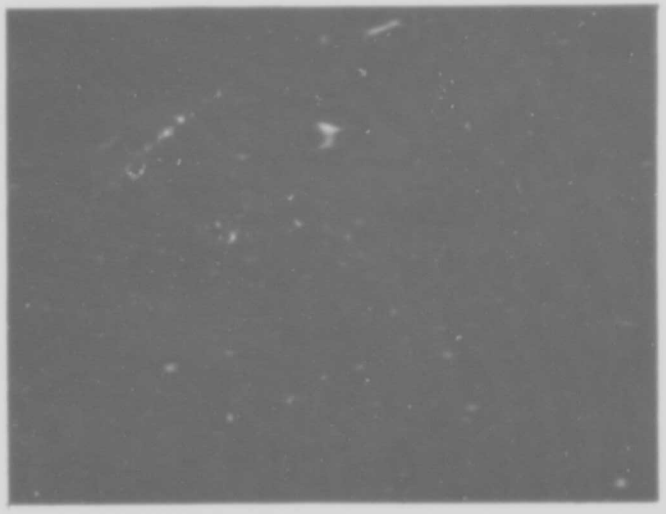

(h)

Fig. 21 (continued)--(e) K K_α intensity picture of this feature; (f) Fe K_α intensity picture of this feature; (g) Ti K_α intensity picture of this feature; (h) Pb M_α intensity picture of this feature

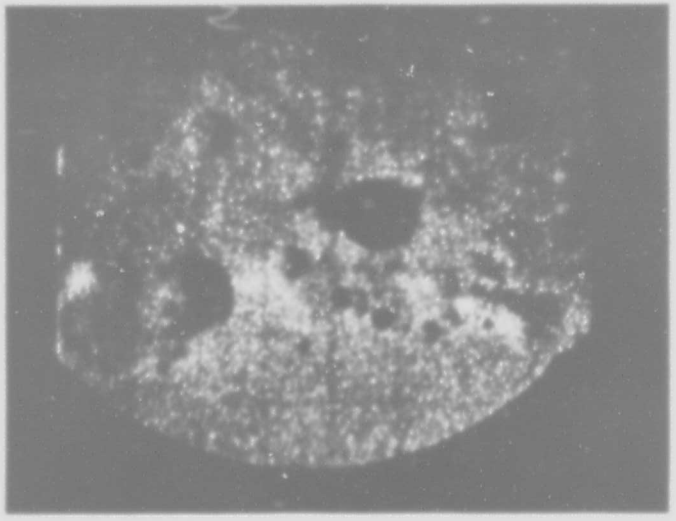

(i)

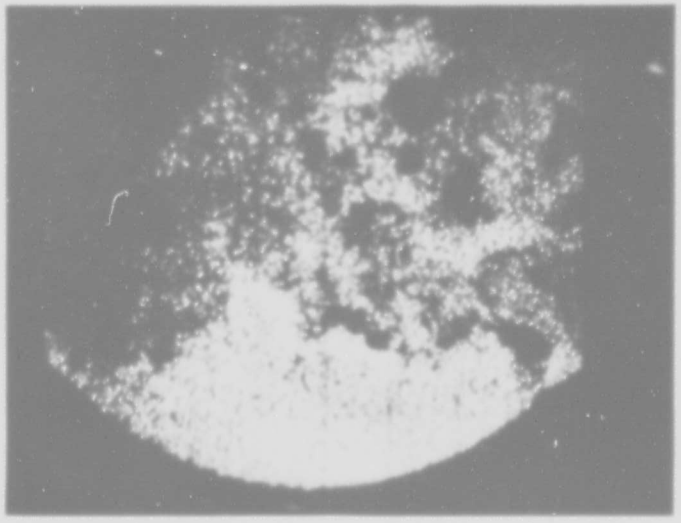

(j)

Fig. 21 (continued)--(i) electron back scatter intensity picture; (j) Fe K_α intensity picture of another feature of this particle

at about the same time as the accretion occurred at the other end. This is shown by the electron back scatter and Fe K_α intensity maps shown in Figs. 21i and 21j, respectively.

The second particle was essentially spherical. It had, however, a small protuberance which undoubtedly was caused by accretion (probably of a particle which itself apparently displays an accretion event) and a neighboring small particle whose connection to the major particle was severed in sectioning the particle. The first surface feature is demonstrated in the photomicrograph and the electron back scatter, Fe K_α, and Pb M_α intensity maps shown in Figs. 22a, 22b, 22c, and 22d. The electron back scatter, Pb M_α, Fe K_α, K K_α, and Si K_α intensity maps for the second surface feature are shown in Figs. 22e, 22f, 22g, 22h, and 22i. The lead boundaries of the two accretion events are quite apparent in the first feature; the iron information appears to be quite similar for both. The second feature is even more interesting. It shows a small lead-coated particle (diameter about 10% of the large particle), which has accreted with a high iron content particle which was also heavily lead coated. The inside of the particle appears to contain regions of nearly pure silica as well. This little particle shows essentially the same features exhibited by the larger particles, that is, those caused by accretion, bulk inhomogeneity, and surface coating.

We have, in addition to the intensity maps, recorded the approximate lead and iron compositions of one of the particles on a chord. Uncorrected percentages of silicon for similar traces have ranged from 20 to 50 for the matrix, and since there are areas where nearly pure SiO_2 exists and the silicon content of SiO_2 is 47%, some reliance can be put on the reported composition. Variations in iron content with depth in the particle, as shown in Fig. 23, range from 15% to 45%, in this case in a somewhat unexpected manner--a precipitous decrease in iron concentration occurs 30 μ from the edge. This may possibly be an accretion effect. Lead contents range from 12% at the surface to undetectable at 60 μ into the ~1000 μ diameter particle. The lead is distributed in a manner suggesting a diffusion profile.

The phenomena governing fallout particle formation seemingly observed in these studies, then, are predominantly those of accretion, solid state diffusion, and possibly cloud inhomogeneity, suggested by the lead coat and/or variation in composition of accreted particles. A strong question of direct applicability of equilibrium chemistry certainly results from this study, although equilibrium chemistry must be considered. However, this study may not be truly representative of events of interest to the Office of Civil Defense, since the fallout particles investigated would appear to be formed in a low energy detonation; that is, the fallout particles would seem to indicate relatively low cloud temperatures for relatively short times. Many of these observations may not be applicable to a much higher energy detonation. A study of particles from larger events, of course, would be desirable.

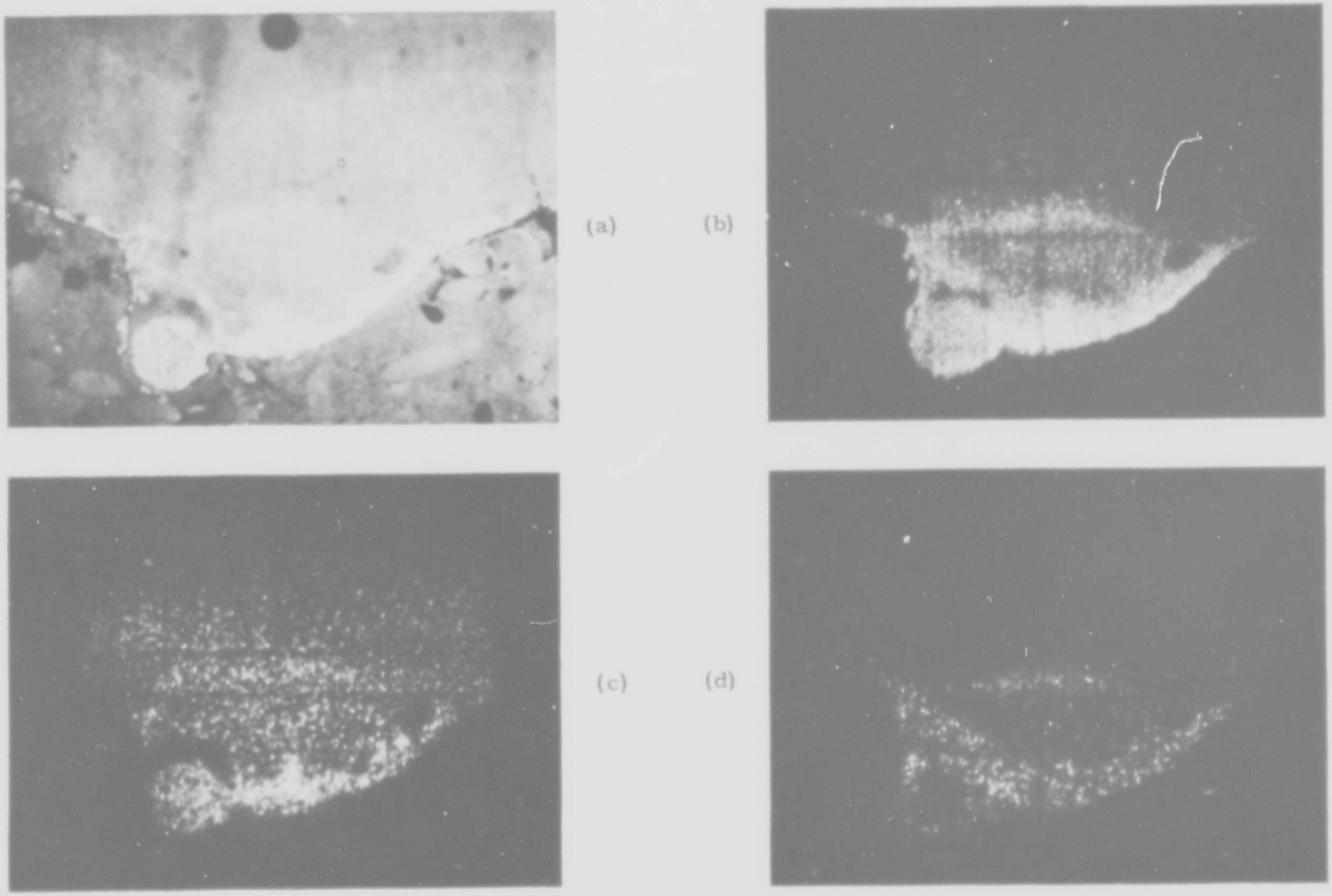

Fig. 22--Microprobe studies of a third particle: (a) photomicrograph of a feature; (b) electron back scatter intensity picture of a feature; (c) Fe K_{α} intensity picture of this feature; (d) Pb M_{α} intensity picture of this feature

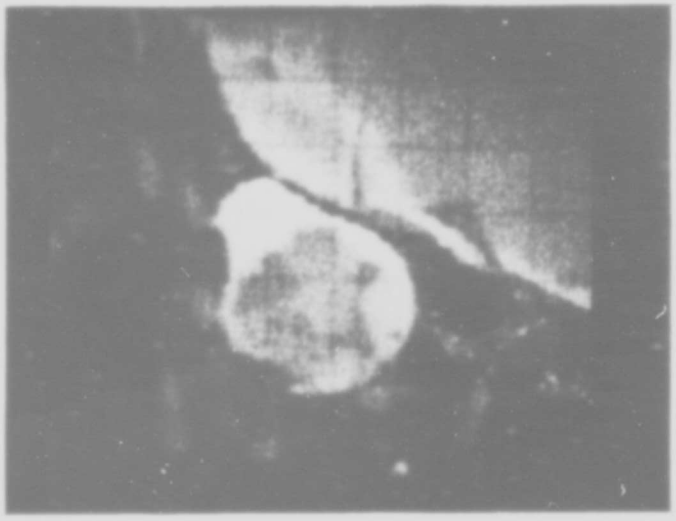

(e)

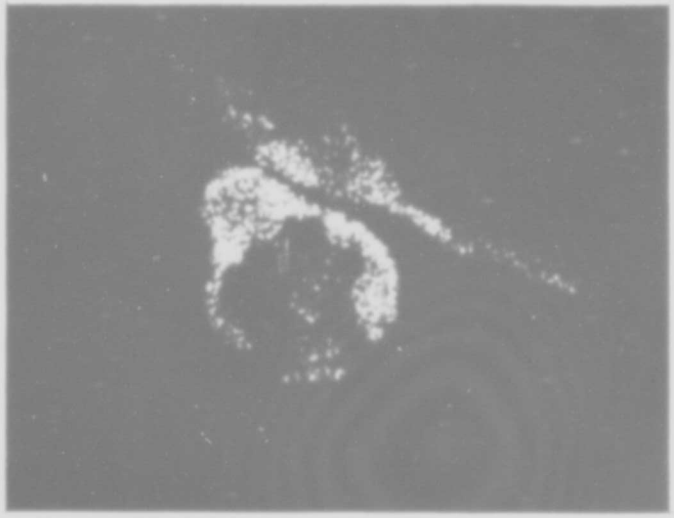

(f)

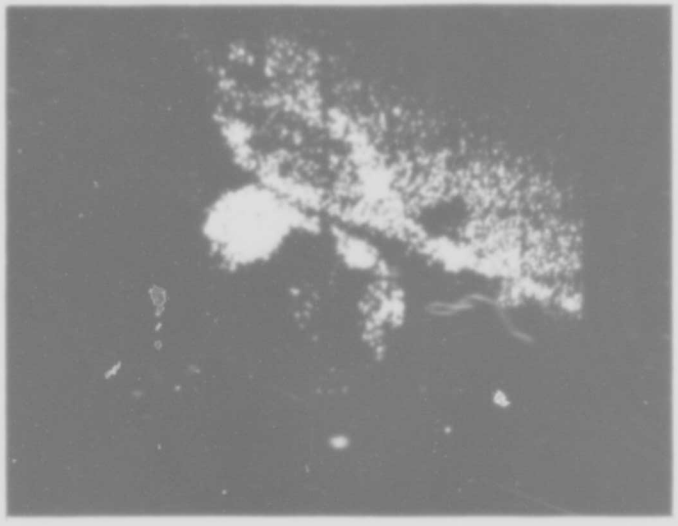

(g)

Fig. 22 (continued)--(e) electron back scatter intensity picture of another feature; (f) Pb M_{α} intensity picture of this feature; (g) Fe K_{α} intensity picture of this feature

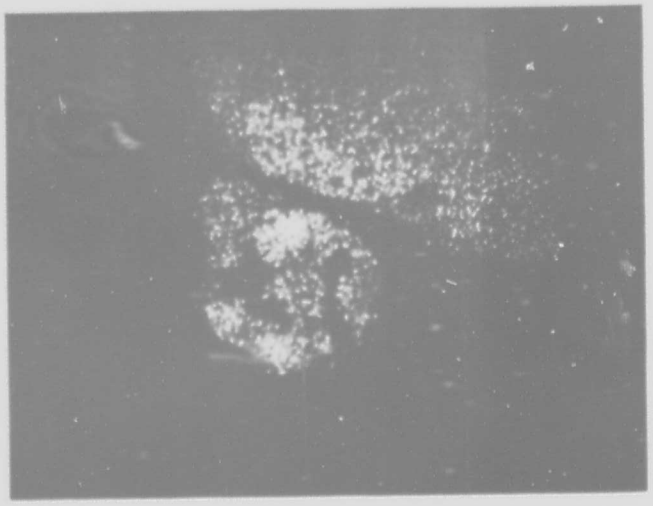

(h)

(i)

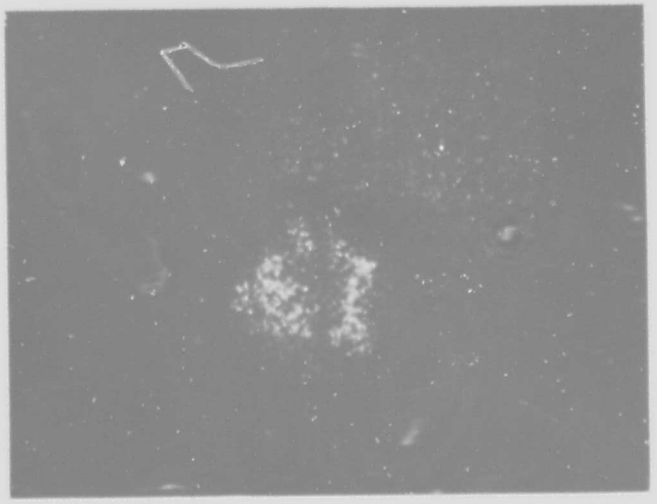

Fig. 22 (continued)--(h) K K_α intensity picture of this feature; (i) Si K_α intensity picture of this feature

BLANK PAGE

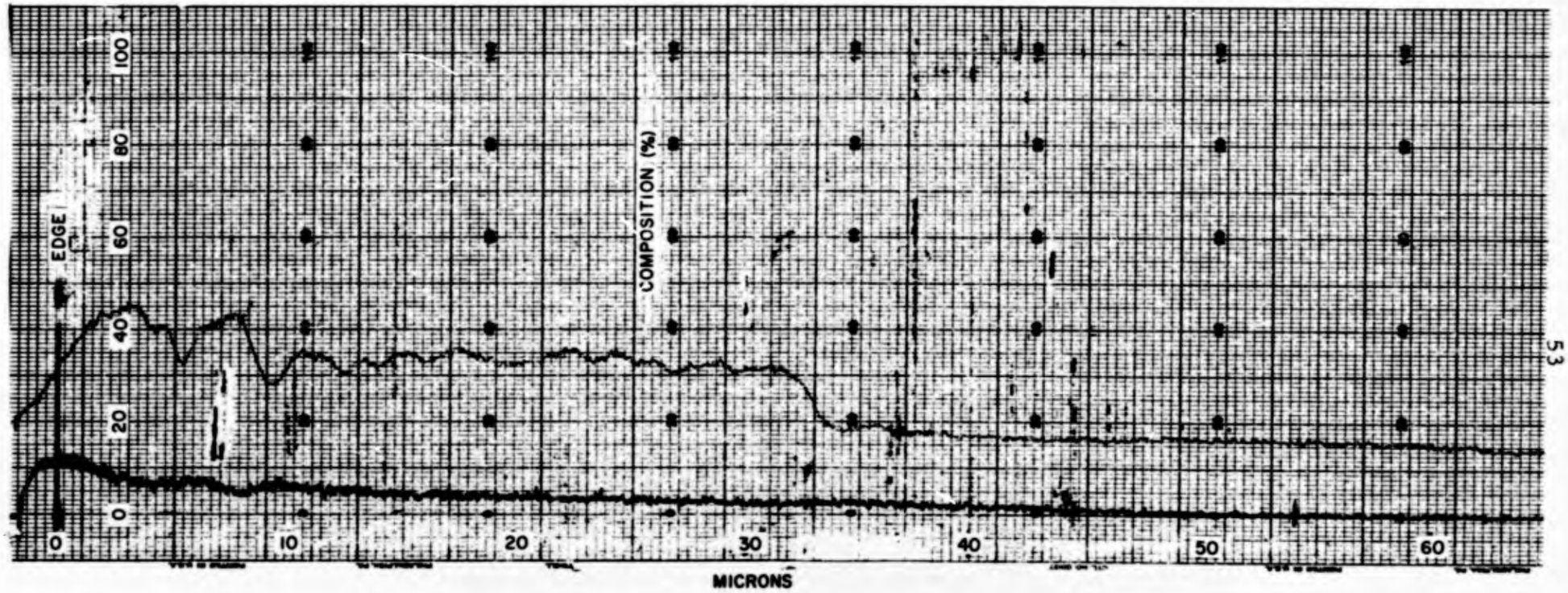

Fig. 23--Microprobe traces following Pb and Fe concentrations from the surface of a fallout particle

VI. FALLOUT MODEL CONSIDERATIONS

Fallout formation falls basically in the realm of phenomena that are describable in kinetic rather than equilibrium terms. The model proposed by C. F. Miller[3] provides the only operational computational system for describing fallout formation. The Miller model is truly a kinetic model in that it involves fast reaction rates between condensed and gas phases (equilibrium conditions) up to a "melting point" of the fallout droplets and infinitely slow interaction between the bulk of the condensed phase and the gas phase afterwards. However, for a process as complex as the formation of fallout, it is unlikely that such a simplified description of kinetics will describe the process well. To aid in improving the Miller model, we have described some points whereby this model departs from realism. These points include the glassy nature of siliceous fallout particles. We have not seen discontinuity or near discontinuity experimentally with glasses in condensed state diffusivity, as does usually occur when liquids solidify. Therefore, no "melting temperature," or for that matter no single temperature, can well describe the kinetic processes occurring during fallout formation. It is also true that liquid silicates, in comparison with liquids in general, comprise a family of substances that are characterized by having high viscosities and low diffusivities. It has been demonstrated in this laboratory that these liquids, well beyond their melting points, will not instantaneously equilibrate with the ambient gas phase. Observations made here suggest that some of the more common-sized fallout droplets should be reasonably far out of equilibrium with the gas phase at their "melting point." For example 10 μ radius particles of CaO-Al_2O_3-SiO_2 eutectic composition in a 1 MT detonation (cooling rate according to Miller[3] is 60°/sec at 1450°K) pick up only 90% of the antimony theoretically absorbable from the cloud while they are at 2000° ±50°K. At temperatures around their "melting point" they would absorb far less (under certain source conditions ~1%) of the antimony absorbable under equilibrium conditions. This example seems typical.

Fallout formation might therefore be described by employing equilibrium absorption data as suggested by Miller, diffusivities as we have indicated, particle sizes, and estimated thermal histories of the particles. Unfortunately, this does not cover all of the kinetic processes occurring during fallout formation. It is believed, for instance, that accretion of particles is important to the description of fission product absorption. The electron microprobe information reported here strongly indicates that the particles investigated were formed from a large number

of smaller particles. If so, the time history of this process must also be considered in a description of fallout formation. This phenomenon will be a function of space densities, velocities, and size of particles.

Another effect that must be considered is that of convection of fission products (stirring) caused by air turbulence exerting a force on the surfaces of a liquid droplet. This possibility became increasingly interesting when it was learned that large toroidal gas velocities are associated with a nuclear cloud. However, calculations by H. G. Norment[20] have suggested that for 10 μ diameter particles, stirring probably is not important because the particle velocities closely match the velocity of the surrounding gas. This is also nearly true for 100 μ diameter particles, but it is not true for 1 mm diameter particles where differences between gas and particle velocities of around 100 ft/sec have been calculated. These large particles, however, are not an important carrier for the radioactivity of the cloud, so convection caused by air turbulence will not be considered further at present.

Summing up, a model describing the formation of fallout should include a chemical description of the absorption of fission products, a nuclear description of the time dependence of the existence of the nuclides, a chemical diffusion representation of movement of nuclides either into or out of the particles, an accretion description to modify the diffusion description, and other phenomena which may be important, such as particle residence time in the nuclear cloud (also only a problem with $\sim$1 mm diameter particles), absorption variation with absorbent, and fission product distributions within the cloud.

VII. EXTENSION OF STUDIES

In the case of cesium absorption, it is apparent that further information on the chemistry involved in the absorption process must be obtained before we can accurately predict the behavior of cesium in fallout. The concentrations studied are much higher than those encountered in fallout formation, and the atmospheric conditions must be studied more thoroughly.

The other systems that we have studied are as uncertain as the cesium system. We have little hope of duplicating fallout conditions (very low fission product pressures, etc.) exactly, but we do have a strong belief that most of the important variables can be studied profitably under attainable experimental conditions. We do expect, therefore, to study these systems to further determine chemical behavior of the species for some fission product systems.

We believe that further consideration of the roles of diffusion and accretion is necessary to produce a more effective fallout model. Some consideration will be given to these phenomena in a continuing program by way of further experimental clarification of diffusion effects and further microprobe investigations of fallout particles.

13. King, J. B., and P. J. Koros, "Diffusion in Liquid Silicates," Conference on the Kinetics of High Temperature Processes, John Wiley and Sons, New York, 1959, p. 80.

14. Stevels, J. M., "The Structure and the Physical Properties of Glass," in Thermodynamics of Liquids and Solids XIII, Springer-Verlag, Berlin, 1962, p. 548.

15. White, J. L., "Thermal Expansion of High Temperature Materials," in Physicochemical Measurements at High Temperatures, Academic Press, Inc., New York, 1959, p. 344.

16. Johnson, J. R., R. H. Bristow, and H. H. Blaur, J. Am. Ceram. Soc. 34, 165 (1951).

17. McCallum, N., and L. R. Barrett, Trans. Brit. Ceram. Soc. 51, 523 (1952).

18. Inghram, M. G., and J. Drowart, "Mass Spectrometry Applied to High Temperature Chemistry," Proc. Intern. Symp. High Temp. Technol., Asilomar Conf. Grounds, Calif., 1959, 219 (1960).

19. Otvos, J. W., and D. P. Stevenson, "Cross Sections of Molecules for Ionization by Electrons," J. Am. Chem. Soc. 78, 546 (1956).

20. Norment, H. G., Technical Operations Research, private communication.

21. Cobine, J. D., Gaseous Conductors, Dover Publications, Inc., New York, 1958, p. 92.

REFERENCES

1. Norman, J. H., and W. E. Bell, "Fallout Studies. High Temperature Interactions Between Gaseous Fission Products and Liquid Silicates. Final Report," General Atomic Report GA-4278, OCD Subtask 3111A, May, 1963.

2. Burns, R. P., et al., J. Chem. Phys. 32, 1363 (1960).

3. Miller, C. F., "Fallout and Radiological Countermeasures I," Stanford Research Institute Project No. IM-4021 (1963), p. 97-168.

4. Bell, W. E., and M. Tagami, "High-Temperature Chemistry of the Ruthenium-Oxygen System," J. Phys. Chem. 67, 2432 (1963).

5. Coughlin, J. P., "Contributions to the Data on Theoretical Metallurgy XII, Heats and Free Energies of Formation of Inorganic Oxides," Bull. 542, Bureau of Mines, Washington, 1954.

6. Bell, W. E., and J. H. Norman, "The High-Temperature Chemistry of Fission Product Elements, Summary Report," USAEC Report GA-5611, General Atomic Division of General Dynamics Corporation, August 1964.

7. Carslaw, H. S., and J. C. Jaeger, Conduction of Heat in Solids, Oxford University Press, London, 1959, p. 234.

8. Yang, L., and M. T. Simnad, "Measurement of Diffusivity in Liquid Systems," in Physicochemical Measurements at High Temperatures, Academic Press, Inc., New York, 1959, p. 304.

9. Owen, A. E., "Electric Conduction and Dielectric Relaxation in Glass," in Progress in Ceramic Science 3, The Macmillan Co., New York, 1963, Ch. 3.

10. Ralkova, J., Silikaty 6, 258 (1962). Also, see J. Ralkova and J. Saidl, "Incorporation of Radioisotopes into Melted Silicates," in Treatment and Storage of High-Level Radioactive Wastes, International Atomic Energy Agency, Vienna, 1963, p. 341.

11. Towers, H., and J. Chipman, J. Metals 9, 769 (1955).

12. Elliott, J. F., M. Gleiser, and V. Ramakrishna, in Thermochemistry for Steelmaking II, Addison-Wesley Publishing Co., Inc., Reading, Pennsylvania, 1963, p. 666.